Diffusion of *n*-type dopants in germanium

Cite as: Appl. Phys. Rev. **1**, 011301 (2014); https://doi.org/10.1063/1.4838215
Submitted: 17 September 2013 • Accepted: 22 October 2013 • Published Online: 02 January 2014

A. Chroneos and H. Bracht

APPLIED PHYSICS REVIEWS

Diffusion of *n*-type dopants in germanium

A. Chroneos[1,2,a)] and H. Bracht[3,b)]
[1]*Engineering and Innovation, The Open University, Milton Keynes MK7 6AA, United Kingdom*
[2]*Department of Materials, Imperial College, London SW7 2AZ, United Kingdom*
[3]*Institute of Materials Physics, University of Münster, Wilhelm-Klemm-Strasse 10, D-48149 Münster, Germany*

(Received 17 September 2013; accepted 22 October 2013; published online 2 January 2014)

Germanium is being actively considered by the semiconductor community as a mainstream material for nanoelectronic applications. Germanium has advantageous materials properties; however, its dopant-defect interactions are less understood as compared to the mainstream material, silicon. The understanding of self- and dopant diffusion is essential to form well defined doped regions. Although *p*-type dopants such as boron exhibit limited diffusion, *n*-type dopants such as phosphorous, arsenic, and antimony diffuse quickly via vacancy-mediated diffusion mechanisms. In the present review, we mainly focus on the impact of intrinsic defects on the diffusion mechanisms of donor atoms and point defect engineering strategies to restrain donor atom diffusion and to enhance their electrical activation. © *2014 AIP Publishing LLC*.
[http://dx.doi.org/10.1063/1.4838215]

TABLE OF CONTENTS

I. INTRODUCTION

Germanium (Ge) has a number of advantages over silicon (Si) or silicon germanium ($Si_{1-x}Ge_x$) alloys including its superior carrier mobilities, low dopant activation temperatures, and smaller band-gap.[1,2] From a technological viewpoint, Ge is more compatible to Si-processes, than other more exotic materials being recently proposed. This has the advantage that existing Si process equipment may be used for Ge device fabrication. Ge appeared in the early days of the semiconductor industry, but it was quickly plagued by the poor quality of germanium dioxide (as compared to silicon dioxide in Si-technology).[1] The introduction of high-*k* gate dielectric materials has eliminated the requirement of a good quality native oxide regenerating the interest of the community for the use of Ge in advanced nanoelectronic devices.

The community aims to develop Ge-based *p*- and *n*-channel metal oxide semiconductor field effect transistors (MOSFET) for advanced high mobility complementary metal-oxide semiconductor (CMOS). As the characteristic dimensions of devices are a few nanometers, the absolute control on the placement of dopants in the Ge substrate, that is, dopant diffusion and dopant-defect interactions, is more important than ever. As fundamental research on Ge was neglected for decades, there are only a few experimental and theoretical studies of impurity diffusion and defect processes in Ge in comparison to Si[3] with most being published over the last decade.[4–21]

Intrinsic point defects such as vacancies (*V*) and self-interstitials (*I*) are the most fundamental atomic vehicles mediating dopant diffusion. Understanding of their properties is necessary to control the diffusion and electrical activation

a)Electronic mail: alexander.chroneos@imperial.ac.uk
b)Electronic mail: bracht@uni-muenster.de

of dopants.[22–34] Earlier investigations of Werner *et al.*[22] determined that *V* mediate self-diffusion in Ge under equilibrium conditions. Under such conditions the concentration of native defects is in thermal equilibrium. No evidence for the existence of *I* have been found under thermal equilibrium but after electron irradiation of Ge first evidence of *I* were obtained by means of perturbed angular correlation spectroscopy.[35] Recent experimental studies and theoretical calculations based on density functional theory (DFT) confirm the dominance of *V* over *I* under thermal equilibrium. This is expressed by the formation energy of the defect that is higher for *I* than for *V*. Accordingly, *V* mainly mediates the diffusion of both *n*- and *p*-type dopants in Ge.[4,36,37] Figure 1 illustrates the diffusion coefficients of the *n*-type dopants phosphorus (P), arsenic (As), and antimony (Sb) and of the *p*-type dopants boron (B), aluminium (Al), gallium (Ga), and indium (In) in comparison to Ge self-diffusion. The diffusion data are representative for dopant diffusion under equilibrium conditions. The diffusion of the *n*-type dopants clearly exceeds the diffusion of the *p*-type dopants. Moreover, donor diffusion exceeds Ge self-diffusion and increases from P to Sb. On the other hand, the diffusion of the *p*-type dopants is very similar to self-diffusion and in the case of B[38–41] even significantly lower.[14,22] The slow diffusion of the acceptor dopants and in particular of B is very advantageous for the formation of ultra shallow acceptor doped regions in Ge.

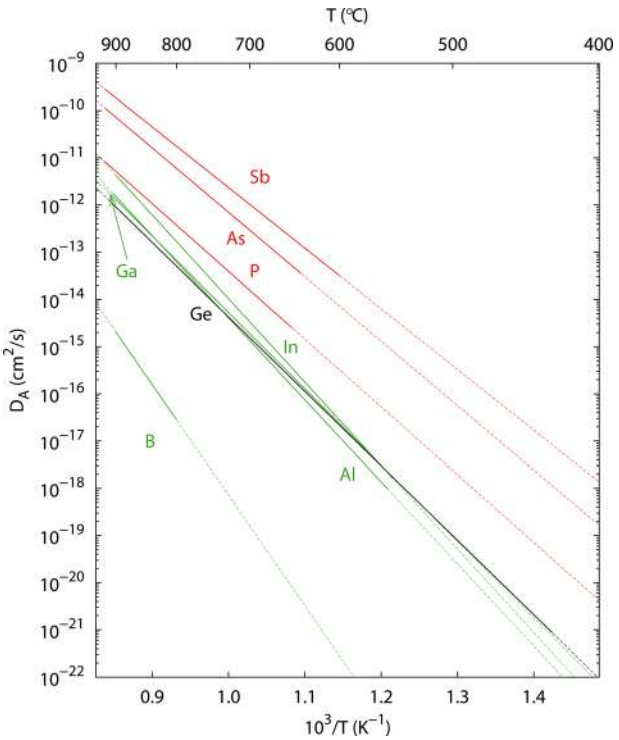

FIG. 1. Diffusion coefficients of the *n*-type dopants (red lines): phosphorus (P),[47] arsenic (As),[47] and antimony (Sb)[47] in Ge compared to Ge self-diffusion (black line)[14] and to the *p*-type dopants (green lines): boron (B),[86] aluminum (Al),[42] gallium (Ga),[85] and indium (In).[45] Diffusion data are representative for dopant diffusion under equilibrium conditions. Each solid line spans the range of the respective experimental results, and the corresponding dashed line indicates an extrapolation to lower and higher temperatures.

The slow diffusion of B is associated with a high diffusion activation enthalpy that exceeds the activation enthalpy of self-diffusion by more than 1 eV. This indicates that B atoms are not likely associated with *V*. This is confirmed by density functional theory (DFT) investigations that reveal that the mobile B*V* pair is unstable.[38,39] The high diffusion activation enthalpy of B rather indicates a diffusion of B via *I*. An *I*-mediated diffusion is supported by the DFT study of Janke *et al.*[38] and experimentally by the enhanced diffusion of B under a *I* supersaturation established by irradiation. Compared to B, the diffusion of the other *p*-type dopants is fully consistent with the vacancy mechanism. The slightly higher diffusion activation enthalpy of Al, Ga, and In[42–45] compared to self-diffusion[14] reflects an interaction of these *p*-type dopants to *V* that is less attractive than in the case of the *n*-type dopants P, As, and Sb. This difference in the diffusion behaviour of *p*- and *n*-type dopants in Ge is likely due to Coulomb interactions between the substitutional dopant and *V* (see Sec. III). For high dopant concentrations $\sim 10^{20}$ cm^{-3} dopant diffusion is not only mediated by *V* via the vacancy mechanism or *I* via the interstitialcy mechanism but also by the formation of dopant-defect clusters.[36] The understanding of cluster formation is fundamental for controlling the diffusion and activation of dopants in the fabrication of Ge-based devices. This, in particular, holds for Ge doped by implantation and subsequent annealing. For example, recent secondary ion mass spectrometry (SIMS) analysis of heavily indium-doped Ge revealed that a high proportion of the indium dose ($\sim$16%) is trapped in a characteristic hump near the surface.[45] A plausible explanation is that in high indium concentration regions In_nV_m clusters form.[46]

Experimental and theoretical studies on donor diffusion have established that *n*-type dopants (A = P, As, Sb) diffuse in Ge via a vacancy mechanism at a faster rate than self-diffusion[36,37,47–49] (see Fig. 1). However, this fast diffusion of donor atoms is unfavorable for the formation of ultra shallow donor profiles. Efficient strategies need to be developed to constrain the diffusion of *n*-type dopants and to increase their level of electrical activation, i.e., to hinder the formation of dopant defect clusters.

This review is mainly focused on the defects and their interaction involved in the diffusion of donor atoms in Ge. In the first part, the diffusion and cluster formation of donor atoms is discussed from an experimental and density functional theory perspective. This is followed by a review of the main point defect engineering strategies (codoping studies, proton irradiation to form self-interstitials) that aim to limit the impact of *V* on the diffusion and deactivation of donor atoms in Ge. Finally, a brief summary and outlook for future directions are given.

II. INTRINSIC DEFECTS AND DEFECT REACTIONS

A. Intrinsic defects

1. Charge states and energy levels

Intrinsic defects in semiconductors such as *V* and *I* form due to thermodynamic principles and can exist in various charge states depending on the position of the Fermi level. *V*

and I are the main vehicles that mediate the diffusion of self- and dopant atoms. In order to fully understand and thus control dopant diffusion and dopant-defect interactions in Ge during device fabrication, the properties of intrinsic defects such as their preferred charge states, their formation and migration enthalpy and entropy, and interactions with dopant atoms must be known.

Self-diffusion studies provide the most direct access to the properties of intrinsic defects. First studies were performed more than 50 years ago.[50,51] The impact of doping and hydrostatic pressure on self-diffusion provided evidence on the acceptor nature of V in Ge.[22] The excellent agreement between Ge self-diffusion and the V contribution to self-diffusion deduced from copper diffusion in dislocation-free Ge proved the dominance of V in Ge.[52–54] More recently, experiments on self-diffusion in Ge have been extended to lower temperatures[14] to verify whether the dominant mechanism of self-diffusion changes as in the case of Si.[55–57] Utilizing isotopically modulated ^{70}Ge/^{nat}Ge multilayer structures, the diffusional intermixing at the ^{70}Ge/^{nat}Ge interface was detected down to 429 °C by means of neutron reflectometry.[14] Self-diffusion data for temperatures between 429 °C and 904 °C[14,22] are accurately described by a single Arrhenius expression with a diffusion activation enthalpy of 3.13 eV and a prefactor of $D_0 = 25.4$ cm^2 s^{-1} (Ref. 14) (see black solid line in Fig. 1). The study reveals that V dominates in Ge even at low temperatures. A contribution of I to self-diffusion is not apparent. Accordingly, self-diffusion in Ge is mainly controlled by one single vacancy form with constant, i.e., temperature independent, vacancy formation, and migration enthalpies (entropies). The concept of extended V first proposed by Seeger and Chik[58] and recently adapted by Cowern *et al.*[59] for diffusion in Si and Ge is not applicable for the vacancy in Ge.

Investigations of Ge self-diffusion under n-type doping evidence that V are doubly negatively charged. This was independently verified by Brotzmann *et al.*[36] and Naganawa *et al.*[12] by dopant diffusion in isotopically controlled Ge multilayers. The impact of p-type doping on Ge self-diffusion was recently investigated with homogenously B-doped Ge isotope structures.[60] Figure 2 illustrates the temperature dependence of self-diffusion in p-type compared to undoped Ge. P-type doping clearly retards self-diffusion compared to electronically intrinsic conditions. The doping dependence of self-diffusion suggests two V-related acceptor levels in the band gap of Ge.[60] The first acceptor level is located 0.28 eV above the valence band maximum (VBM) and the second level at 0.14 eV above VBM. This level ordering is inverted, i.e., the single acceptor state lies above the double acceptor state. This is indicated in the inset of Fig. 2. As consequence of the level ordering, doubly negatively charged V^{2-} prevails under n-type doping and neutral V^0 under p-type doping. Singly charged V^- do not dominate and control self-diffusion under any doping level.[60] This is illustrated in Fig. 3 by the individual contributions of neutral, singly, and doubly negatively charged V to the total Ge self-diffusion coefficient at 700 °C deduced from the doping dependence of self-diffusion.

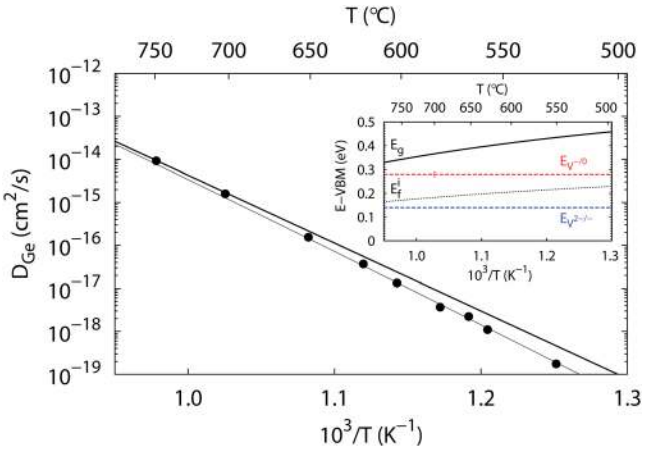

FIG. 2. Self-diffusion in Ge as function of the inverse temperature for electronically intrinsic (thick solid line in Ref. 14) and p-type doping conditions (●, thin solid line in Ref. 60). The inset illustrates the positions of the V-related energy levels (dashed lines) deduced from the doping dependence of self-diffusion. Expressions given by Ref. 100 were considered for the temperature dependence of the band gap $E_g(T)$ (solid line) and the position of the intrinsic Fermi level E_f^i ($\sim 0.5E_g(T)$) (short-dashed line).

The energy level scheme of V is consistent with recent results of deep level transient spectroscopy (DLTS) studies on defects introduced in Ge by low-temperature electron irradiation.[61] Present theoretical calculations do not predict an inverse level ordering of the first and second acceptor states (see Sec. III). But an inverse ordering cannot be excluded[62] because theoretical results are representative for 0 K and it remains unclear how the level positions depend on temperature.

Diffusion studies under equilibrium conditions all indicate that Is do not significantly contribute to the atomic transport in Ge. However, I can be formed non-thermally, e.g., by electron irradiation. Haesslein *et al.*[35] identified a donor level at 0.04 eV below the conduction band of Ge in electron irradiated Ge by means of perturbed angular correlation (PAC) spectroscopy. They attributed this level to I.

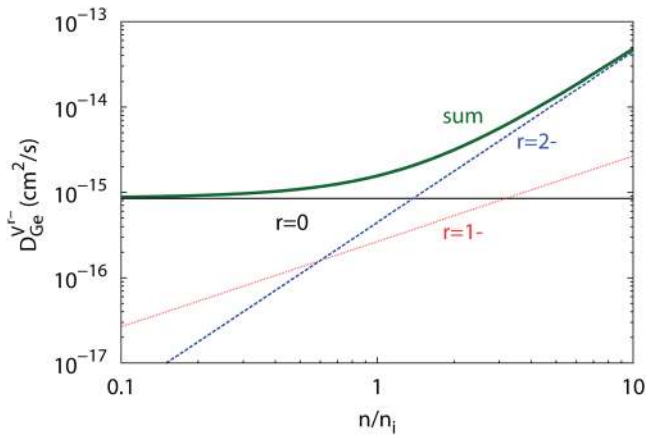

FIG. 3. Individual contributions of neutral (r = 0: thin black solid line), singly (r = 1: red short-dashed line), and doubly (r = 2: blue dashed line) negatively charged V^- to Ge self-diffusion at 700 °C. The total Ge self-diffusion coefficient is given by the sum of the individual contributions and shown by the green thick solid line. The singly negatively charged V^- does not dominate self-diffusion under any doping level.

According to their work, self-interstitials introduce donor and the vacancy acceptor states.

The disparity in the electronic property of I and V is likely the origin of the efficient recombination of V and I introduced, e.g., by implantation. Implantation damage and I-related defect clusters dissolve readily and recrystallization of amorphized Ge proceeds rapidly even at 400 °C.[63–66] This suggests an I–V recombination that is more efficient than in the case of Si, where implantation damage is less effectively removed by means of post-implantation annealing.

2. Thermodynamic properties

Recent Ge self-diffusion studies yield a diffusion activation enthalpy of Q = 3.13 eV.[14] This enthalpy equals the sum of V formation and migration. Studies on Cu precipitation in Ge and on thermally induced acceptors formed after quenching reveal a V formation enthalpy of about 2 eV.[24,67–69] Metal diffusion studies of Giese *et al.*[25] support the results of the former quenching experiments. Recently, Vanhellemont *et al.*[26] report a best estimate of (2.35 ± 0.1) eV and (0.6 ± 0.1) eV for the formation and migration enthalpy of V, respectively, which is based on available experimental and theoretical results. A formation energy around 3 eV is predicted by theory for I.[23,26,70] The higher formation energy of I compared to V explains the lower I concentrations under thermal equilibrium.

Calculated migration energies vary between 0.3 and 1.2 eV depending on the charge state of I.[71] The highest migration enthalpy of 1.2 eV is predicted for the doubly positively charged I^{2+}.[71] Recent investigations of radiation-enhanced self- and boron diffusion in Ge provide a value of (1.84 ± 0.26) eV for the migration enthalpy of I.[72] Considering the electronic property of I in Ge induced by irradiation and measured by DLTS and PAC[35,61] the experimentally determined migration enthalpy of 1.84 eV is assigned to the doubly positively charged I^{2+}.[72] The theoretical prediction of 1.2 eV reported by Carvalho *et al.*[71] is in acceptable agreement with the experimental value.

Experimental and theoretical results on V and I consistently show the dominance of V under thermal equilibrium conditions. Vacancies are doubly negatively charged under n-type doping and neutral under p-type doping. Self-interstitials are not relevant for self- and dopant diffusion under thermal equilibrium. However, their impact on atomic transport in Ge strongly changes under non-equilibrium conditions (see Sec. V).

B. Defect reactions

The interaction of intrinsic defects with mainly substitutionally dissolved foreign atoms promotes the diffusion of dopants. The direct exchange of dopants with adjacent host atoms is energetically too costly and thus not relevant for dopant diffusion in Ge. Considering both V and I to be involved in dopant-defect interactions, the following reactions describe in general the diffusion of dopants in semiconductors:

$$AV \leftrightarrow A_s + V, \tag{1}$$

$$AI \leftrightarrow A_s + I, \tag{2}$$

$$AV + I \leftrightarrow A_s, \tag{3}$$

$$AI + V \leftrightarrow A_s. \tag{4}$$

AX represents the dopant-defect pair with X = {V, I} and A_s the substitutional dopant. Reactions (1) and (2) are denoted the vacancy and interstitialcy mechanisms of dopant diffusion, respectively, and reactions (3) and (4) the dopant-defect pair assisted recombination of X. Each defect considered in reactions (1) to (4) can exist in a specific or even in various charge states. For clarity, the charges states of the defects are not indicated by superscripts. A more general treatment of the defect reactions is given in Ref. 73. It is evident that the mathematical description of reactions (1) and (2) as well as of reaction (3) and (4) is very similar. Reaction (2) is also representative for the kick-out mechanism in the case the AI pair is substituted by an interstitial dopant A_i. Similarly, reaction (4) also describes the Frank-Turnbull or dissociative mechanism ($A_i + V \leftrightarrow A_s$) of foreign atoms that occupy both interstitial and substitutional lattice sites. Reactions (1) to (4) describe an effective diffusion of the dopant A via the formation of a mobile dopant-defect pair. As for a general chemical reaction, the formation of A_s is either controlled by the supply of AX or the removal of X. In the case the supply of AX limits the formation of A_s, the effective diffusion of A is called foreign-atom controlled.[73] On the other hand, the native defect controlled mode of dopant diffusion exists when the removal of X limits the formation of A_s.[73] The diffusion of group III and V elements in Ge is fully characteristic of a foreign-atom controlled diffusion mode. A prominent example for the native defect controlled mode is the diffusion of copper in Ge, which is consistently described on the basis of the dissociative mechanism that was first proposed by Frank and Turnbull in 1956.[74] Reactions (1) to (4) are the most fundamental mechanisms that describe the diffusion of mainly substitutionally dissolved dopants via interaction with isolated vacancies and self-interstitials. Of course, more complex native defects such as di-, tri-, and higher order V and I clusters can, in principle, contribute to self- and dopant diffusion, but the low concentration of isolated intrinsic defects in Ge under thermal equilibrium conditions leads to a low probability for the formation of higher order defect clusters. In the case of Ge, the formation of such defect clusters is also hindered by Coulomb interactions between the same types of intrinsic defects as both V and I possess high charge states for a wide range of doping levels. This situation changes drastically when dopant atoms are introduced by implantation and are activated by subsequent annealing. However, the processes taking place during implantation and post-implantation annealing are quite complex and hardly understood in all details. More defined non-equilibrium conditions are realized by concurrent annealing and irradiation. The defect reactions in Ge relevant for such conditions are treated in Sec. V.

In contrast to aggregates of intrinsic defects, dopant-defect complexes can also form under equilibrium conditions. Driving forces are elastic and electrostatic interactions,

i.e., a reduction in local strain energy or a Coulomb attraction among differently charged defects. By all means, the formation of dopant-defect complexes is highly undesirable during device fabrication. It reduces the concentration of electrically active dopants and the mobility of free carriers due to scattering events. It is therefore of pivotal interest to understand the mechanisms that lead to dopant deactivation in order to develop efficient strategies for its prevention.

The simplest reactions that initiate the formation of dopant-defect complexes are

$$AX + A_s \leftrightarrow A_2X, \quad (5)$$

$$AX + X \leftrightarrow AX_2. \quad (6)$$

These reactions describe a dopant-defect pair AX that gets close to a substitutional dopant or to an isolated intrinsic defect X. A_2X and AX_2 are the respective defect complexes consisting of either two dopant atoms or two native defects. The relevance of these reactions for *n*-type dopants in Ge is discussed in Sec. III A, and differences to the diffusion behavior of *p*-type dopants are highlighted. Certainly, more complicated dopant-defect clusters can evolve when additional mobile defects such as AX and X approach the complex. However, it is beyond the scope of this review to describe the evolution or dissolution of bigger clusters as this has been performed, e.g., for B-interstitial clusters (BICs) in Si.[75–77] The A_2X and AX_2 complexes are considered as the nucleus of bigger defect clusters. Accordingly, the formation of big defect clusters is hindered when the formation of the defect nucleus is suppressed.

III. DONOR ATOM DIFFUSION

A. Experimental evidence for the vacancy mechanism

Experiments on the diffusion of *n*-type dopants such as P, As, and Sb in Ge have revealed the dominance of singly negatively charged dopant-*V* pairs.[47] In Si, the corresponding dopant-*V* pairs are mainly neutral. Only for very high doping levels a contribution due to singly negatively charged dopant-*V* pairs becomes evident in, e.g., P diffusion profiles (see, e.g., in Ref. 78). This difference in the preferred charged states of dopant-*V* pairs explains the strong doping dependence of the diffusion of *n*-type dopants in Ge that increases with the square of the electron concentration.[47] The doping dependence of donor diffusion is illustrated in Fig. 4 for As diffusion in Ge at 820 °C for 6000 s. Different As vapor pressures were realized in the diffusion experiment in order to establish low and high As doping levels at the Ge surface (see Ref. 47 for details). It is evident from Fig. 4 that the doping level strongly affects both the shape and penetration depth of the As profile. The lower profile shown in Fig. 4 reflects a doping level of about $10^{17}\,cm^{-3}$, which is below the intrinsic carrier concentration at the diffusion temperature. In this case, the dopant profile is described by the concentration independent intrinsic As diffusion coefficient.[47] The upper profile reflects a doping level that exceeds the intrinsic carrier concentration, i.e., extrinsic doping conditions are realized. In this case, a concentration dependent

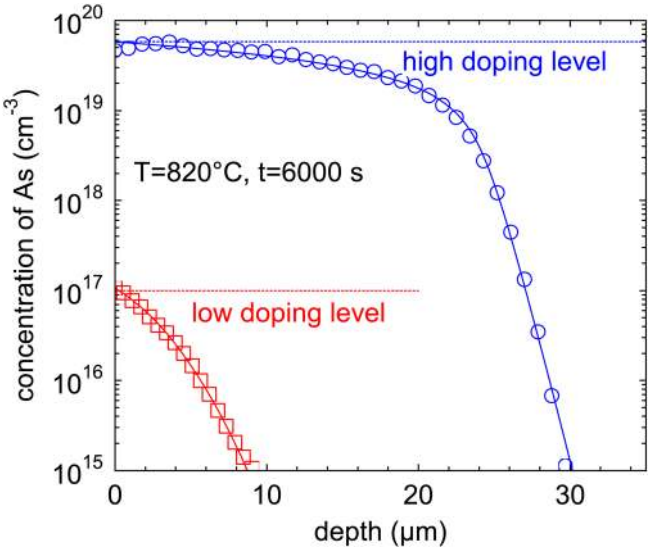

FIG. 4. Concentration profiles of As measured by means of the spreading resistance technique after diffusion annealing at 820 °C for 6000 s.[47] The profiles demonstrate the strong doping dependence of As diffusion established by different As surface concentrations.

dopant diffusion profile develops, which is specific to the charges states of the defects involved in the diffusion process. The same diffusion behavior is observed for P and Sb in Ge.[47] The interrelation between the intrinsic $D_A(n_i)$ and extrinsic $D_A(n)$ donor diffusion coefficient is given by[47]

$$D_A(n) = D_A(n_i) \cdot (n/n_i)^2, \quad (7)$$

where n_i and n are the intrinsic and free carrier concentration. Whereas the doping dependence of donor diffusion in Ge increases with the square of the electron concentration, *n*-type dopant diffusion in Si only increases with the electron concentration.[78]

In summary, the diffusion of *n*-type dopants A = {P, As, Sb} in Ge is accurately described by the vacancy mechanism with the following defects and charge states involved:[47]

$$AV^- \leftrightarrow A_s^+ + V^{2-}. \quad (8)$$

The diffusion of donor atoms A proceeds via mobile A*V* pairs. Their dissociation leads to the formation of substitutional dopants A_s and *V*. The charge state of the A*V* pair becomes visible in the doping dependence of diffusion[47] and the charge state of *V* by experiments on the simultaneous self- and dopant diffusion in isotopically controlled Ge multilayers.[12,36] Moreover, the dopant diffusion mode, i.e., foreign-atom or native-defect controlled, becomes evident in the correlation between the diffusion coefficients derived from self- and dopant diffusion and the shape of the dopant diffusion profiles. The way to characterize the mechanisms of dopant diffusion in semiconductors is described in detail in Ref. 73.

The strong doping dependence of donor diffusion is generally supported by numerous experimental studies on the diffusion of *n*-type dopants in Ge. Vainonen-Ahlgren *et al.*[79] studied As diffusion in Ge from a GaAs overlayer. Although their interpretation of As diffusion is misleading (see Ref. 4),

the experiments clearly demonstrate a strong doping dependence of As diffusion. Further experiments reported in the literature on donor diffusion in ion-implanted Ge also consistently support the strong doping dependence of diffusion.[41,80–84] These studies confirm the dependence of donor diffusion on the square of the free carrier concentration. However, implantation damage gives rise to enhanced donor diffusion, in particular, at short diffusion times.[83] Accordingly, diffusion data deduced from implanted and annealed samples are often not representative for equilibrium diffusion conditions. In this respect, the P diffusion data reported by Chui *et al.*[41] that clearly exceed the equilibrium intrinsic diffusion coefficient of P (Ref. 80) more likely reflect a transient enhanced diffusion due to implantation damage than an equilibrium P diffusion.

Compared to the diffusion of donor atoms in Ge, the diffusion of acceptor atoms behaves very different. The diffusion of In and Ga does not show any significant doping dependence.[45,85] This demonstrates that InV and GaV pairs must be singly negatively charged and therewith possess the same charge state as the In and Ga acceptor. Presumably, Al in Ge behaves similar.[42] Hence, the following defects and charges states are involved in the diffusion of p-type dopants A = {Al, Ga, In} via the vacancy mechanism:

$$AV^- \leftrightarrow A_s^- + V^0. \quad (9)$$

The dominance of the neutral vacancy under p-type doping was evidenced by the doping dependence of Ge self-diffusion.[60]

The activation enthalpy of P, As, and Sb diffusion for electronically intrinsic and thermal equilibrium conditions was determined by Brotzmann and Bracht[47] from the temperature dependence of the dopant diffusion coefficient (see Fig. 1). They report values of 2.85 eV, 2.71 eV, and 2.55 eV for P, As, and Sb, respectively. The experimental results indicate a decreasing activation enthalpy with increasing dopant size. This dependence is supported by theoretical results (see below) and reflects a binding energy of the AV pair that increases with increasing dopant size. The higher the binding energy, the higher will be the probability that a vacancy stays close to the dopant atom and mediates dopant diffusion via a vacancy ring mechanism (see Sec. III D). In the case of n-type dopants, the formation of AV pairs is favored by Coulomb attraction between the singly positively charged donor atom A_s^+ and the doubly negatively charged V^{2-}. For p-type dopants Al, Ga, and In, the formation of the mobile AV^- pair is not favored by Coulomb interaction. Accordingly, acceptor diffusion is slower than donor diffusion (see Fig. 1), and the diffusion activation enthalpies of the p-type dopants clearly exceed those of the n-type dopants.

A striking exception is the diffusion of B in Ge. The diffusivity of B is several orders of magnitude lower than self-diffusion (see Fig. 1) and described with a diffusion activation enthalpy of 4.65 eV[86] that clearly exceeds the activation enthalpy of 3.13 eV determined for self-diffusion.[14] On the one hand, the high activation enthalpy of B diffusion indicates that the interaction between B and V must be repulsive. Such a repulsive interaction is supported by theoretical calculations.[39] On the other hand, the high activation enthalpy and associated slow diffusion of B can also reflect a I-mediated diffusion via the interstitialcy mechanism (2).[72,87]

B. Experimental evidence for donor deactivation

It is now generally accepted that the diffusion of donor atoms in Ge occurs via the vacancy mechanism (1), i.e., via mobile AV pairs. However, for dopant concentrations close to $10^{20}\,cm^{-3}$ donor diffusion is at variance with the vacancy mechanism (1).[36] This becomes evident in chemical dopant profiles that deviate from the expected box shape predicted by reaction (8). These dopant profiles reveal a lower concentration of electrical active dopants compared to the chemical dopant profile.[36] The difference between electrical active and chemical dopant concentrations suggests the formation of neutral dopant-defect complexes. Considering the charge states of substitutional donors A_s^+ and AV^- pairs the formation of dopant-defect complexes is favored by Coulomb interaction. Indeed taking into account the reaction

$$AV^- + A_s^+ \leftrightarrow A_2V^0, \quad (10)$$

that describes the formation of a neutral dopant-defect complex A_2V, the diffusion and electrical activation of donor atoms in Ge for high dopant concentrations is consistently described by means of reactions (8) and (10).[36] Note, the relevance of reaction (10) and their defects involved is hardly proved by spectroscopic studies that are generally performed *ex-situ* after diffusion annealing. During cooling, more complex defect clusters may form that hamper a clear detection of A_2V. On the other hand, the chemical dopant profile measured with SIMS shows the distribution of dopant atoms established during diffusion annealing and stored by quenching. The dopant distribution reflects the dopant diffusion behavior and provides information about possible defects involved in the diffusion process.

The overall consistent interpretation of donor diffusion in Ge based on reactions (8) and (10) supports the relevance of A_2V in the diffusion process. Certainly, higher order A_mV_n defect clusters develop when additional AV pairs join the A_2V complex. The formation of such higher order clusters is favored during slow cooling from high temperatures and post-implantation annealing at low temperatures. High temperature treatments rather dissolve A_mV_n clusters.

Reaction (10) not only describes the formation of a dopant-defect cluster but also the direct deactivation of the donor. An interaction between AV and V via reaction (6) can also lead to dopant-defect clusters and donor deactivation (indirectly via $As_s + V \rightarrow AV$). In the case of n-type dopants in Ge, however, the formation of AV_2 via reaction (6) is not likely as both AV pairs and isolated V are negatively charged, and Coulomb repulsion is expected to suppress the formation of dopant-defect clusters.

The enhanced diffusion of donors with increasing doping level and their electrical deactivation are both highly undesirable for device fabrication that aims for shallow dopant profiles with a maximum active dopant concentration. Considering reactions (8) and (10), the technological

requirements of shallow and heavily donor doped regions are fulfilled when high processing temperatures for short times are realized. High temperature treatments suppress the formation of dopant-defect clusters, and short annealing times limit the penetration of the dopants introduced beforehand by, e.g., ion implantation. Thereby enhanced diffusion due to implantation damage is also suppressed. For example, Wündisch *et al.*[64,88] have demonstrated by millisecond flash lamp annealing of shallow P implants that an electric active P concentration of about $6.5 \times 10^{19}\,\mathrm{cm}^{-3}$ can be realized without noticeable P diffusion. Similarly, high concentrations of electrically active As and Sb were obtained by laser annealing of As- and Sb-implanted Ge.[89] The short laser anneals favor solid phase epitaxial regrowth (SPER), i.e., the recrystallization of Ge layers that were amorphized by ion implantation either beforehand by means of Ge implantation or by dopant implantation itself. In particular, laser annealing is advantageous as even structural defects can be removed that are hardly dissolved by conventional thermal treatments (see, e.g., Bruno *et al.*[89]). Since device fabrication processes are aiming for shallow dopant profiles with high level of electrical activation, post-implantation laser or flash lamp annealing of donor implanted Ge turns out to be more advantageous than rapid thermal annealing (RTA). This is, e.g., demonstrated by laser thermal processing of P-implanted Ge for the formation of n+/p junctions.[7,80,90] Laser annealing above the melting threshold followed by SPER eliminates implantation damage and reduces donor diffusion to the Ge surface and bulk, which would limit the maximum doping level. On the other hand, RTA treatments at low processing temperatures are also sufficient to remove implantation damage and to suppress donor diffusion as demonstrated by Satta *et al.*[63] and Chui *et al.*,[91] but the low processing temperatures required to limit donor diffusion will favor the formation of dopant-defect complexes and thus donor deactivation. Accordingly, short anneals at high temperatures realized by flash lamp and laser annealing are very beneficial for the realization of ultrashallow junctions with high active dopant concentrations.

C. Experimental evidence for defect engineering strategies

In addition to the abovementioned short-time high-temperature treatments other strategies to suppress donor diffusion and to maximize their activation concern, e.g., the impact of codoping with other elements or non-equilibrium diffusion conditions realized by irradiation. All these concepts have in common that they aim to suppress the formation of AV pairs that mediate both the diffusion and deactivation of donors (see reaction (8) and (10)). Defect reactions operative under non-equilibrium diffusion conditions realized by irradiation are treated in Sec. V. The impact of codoping on the diffusion of n-type dopants has been evidenced, e.g., for carbon.[36,92] Carbon is an isovalent impurity and possesses a very low solubility in Ge ($[\mathrm{C}] \leq 2.5 \times 10^{14}\,\mathrm{cm}^{-3}$ (Ref. 93)). However, carbon concentrations well above the solubility limit can be introduced by means of epitaxial layer growth. The impact of carbon on As diffusion in Ge is illustrated in Fig. 5. Arsenic diffusion in Ge with alternating undoped and carbon doped layers is clearly retarded compared to As diffusion in undoped Ge. Arsenic aggregation is observed within the Ge layers doped with carbon to concentrations of about $10^{20}\,\mathrm{cm}^{-3}$. The dopant aggregation fully correlates with the carbon profile. Successful modeling of the chemical As profile is achieved on the basis of reactions (8) and (10) and[36]

$$\mathrm{As}V^{-} + \mathrm{C_s}^{0} \leftrightarrow C\mathrm{As}^{0} + \mathrm{e}^{-}. \tag{11}$$

Reaction (11) describes the trapping of negatively charged $\mathrm{As}V^{-}$ pairs by neutral substitutionally dissolved carbon. In the course of this reaction, CVAs complexes are formed. The stability of carbon-vacancy-dopant CVA complexes is confirmed by DFT calculations (see below). Figure 5 also shows the individual contributions of $\mathrm{As_s}$, $\mathrm{As_2}V$, and CVAs to the total As profile (black solid line). At 600 °C, the concentration of substitutional $\mathrm{As_s}$ is about $10^{19}\,\mathrm{cm}^{-3}$, whereas the concentration of $\mathrm{As_2}V$ is a factor of six higher close to the surface. Within the carbon doped Ge layers neutral CVAs complex dominates $\mathrm{As_s}$ increasing the fraction of non-electrically active As.

The codoping study clearly demonstrates that AsV pairs are trapped by carbon. As a consequence, the penetration depth of As diffusion profiles is significantly reduced. Similarly, carbon codoping also reduces the diffusion of P and Sb.[36] A retarded diffusion of donors by carbon is very

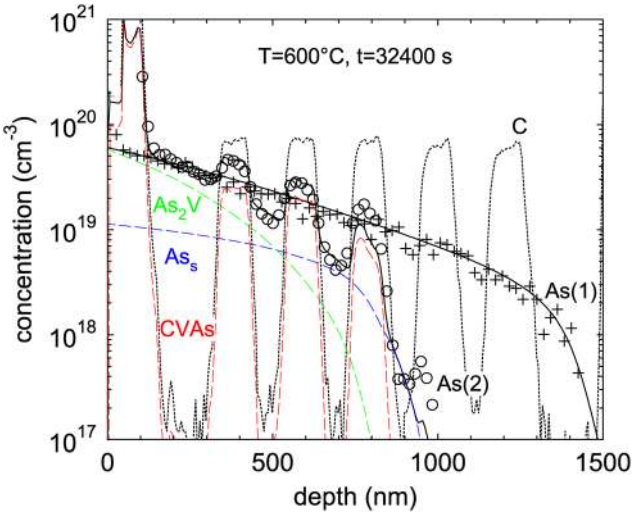

FIG. 5. Concentration profiles of arsenic in natural Ge (As(1)) and carbon codoped Ge (As(2)) measured with SIMS after diffusion annealing at the temperature and time indicated. The diffusion of As in natural Ge (As(1)) is accurately described by reactions (8) and (10) as demonstrated by the solid line. Codoping of Ge with carbon suppresses the diffusion of As as demonstrated by the reduced penetration depth of the As(2) compared to the As(1) profile. Accurate modeling of As diffusion in carbon doped Ge is achieved on the basis of reactions (8), (10), and (11). The latter reaction describes the aggregation of As within the carbon doped Ge layers. The individual contributions of substitutional $\mathrm{As_s}$, the dopant-vacancy complex $\mathrm{As_2}V$, and the carbon-vacancy-dopant complex CVAs to the chemical As profile (see solid line of As(2)) are given by, respectively, the blue, green, and red long dashed lines. The short black dashed line shows the distribution of carbon in the codoped Ge sample after annealing. This profile equals the distribution of carbon in the as-grown material, i.e., no significant diffusion of carbon is observed for the applied annealing conditions.

beneficial for the fabrication of ultra shallow dopant profiles. However, donor deactivation due to the formation of A_2V complexes is not suppressed. In fact, the additional formation of neutral CVA complexes further limits the activation of donors.

Other defect engineering strategies are required to suppress the diffusion and deactivation of *n*-type dopants. Based on reactions (8) and (10), mobile AV pairs are involved both in the diffusion and the deactivation of donors. Accordingly, defect engineering strategies should aim to reduce the concentration and mobility of AV pairs. At a given concentration of substitutional dopants A_s and local equilibrium conditions,[73] the concentration of AV pairs is linked to the concentration of free vacancies, i.e., lower concentrations of V will force lower concentrations of AV pairs. Trapping of V in energetically stable defect clusters can reduce the free vacancy concentration, but it is noted that the equilibrium V concentration can be readily established via in-diffusion of V from free surfaces. The corresponding vacancy diffusivity D_V is several orders of magnitude faster than the V-mediated Ge self-diffusion coefficient $D_{Ge} = 0.5C_V^{eq}D_V/C_0$ (see, e.g., Ref. 54) because the ratio of the V concentration in thermal equilibrium and the Ge atom density is $C_V^{eq}/C_0 < 10^{-7}$ assuming C_V^{eq} data reported by Vanhellemont *et al.*[26] In order to establish a stable undersaturation of vacancies rather a supersaturation of self-interstitials is required. Since self-interstitials in Ge are negligible under thermal equilibrium conditions, other strategies are required to introduce I and therewith to alter the concentration and distribution of vacancies (see Sec. V).

D. Insights from DFT on donor diffusion

It is established that donor atoms (P, As, Sb) in Ge diffuse via V-mediated diffusion mechanisms.[37,42,47,49,85] This is consistent with vacancies being the dominant point defect in Ge. In essence, the singly positively charged donor atom is attracted to the doubly negatively charged V. The doubly negatively charged V in Ge was calculated by Tahini *et al.*[49] to have the lowest formation energy under *n*-type doping conditions. The calculation of the energetics of dopant diffusion in Ge is complicated by the severe underestimation of its band gap due to the incomplete description of the exchange-correlation. Popular DFT approaches such as the local density approximation (LDA) or the generalized gradient approximation (GGA) predict Ge to be metallic. Hybrid DFT calculations employing, for example, the Heyd-Scuseria-Ernzerhof (HSE06) functional[94] can overcome these issues; however, they are computationally very expensive. Another way to correct the band gap is by using the GGA+U approach. Figure 6 represents the band structure of Ge using the GGA, GGA+U, and HSE06 approaches.[49] As it is expected using GGA there is no indirect band gap (refer to Fig. 6(a)), whereas experimentally, it should be 0.74 eV at 0 K.[95] GGA+U and HSE06 approaches predict indirect band gaps of 0.67 eV and 0.85 eV, respectively (refer to Figs. 6(b) and 6(c)).[48] Additionally, the electronic structures of the GGA+U and HSE06 approaches are very similar.[49]

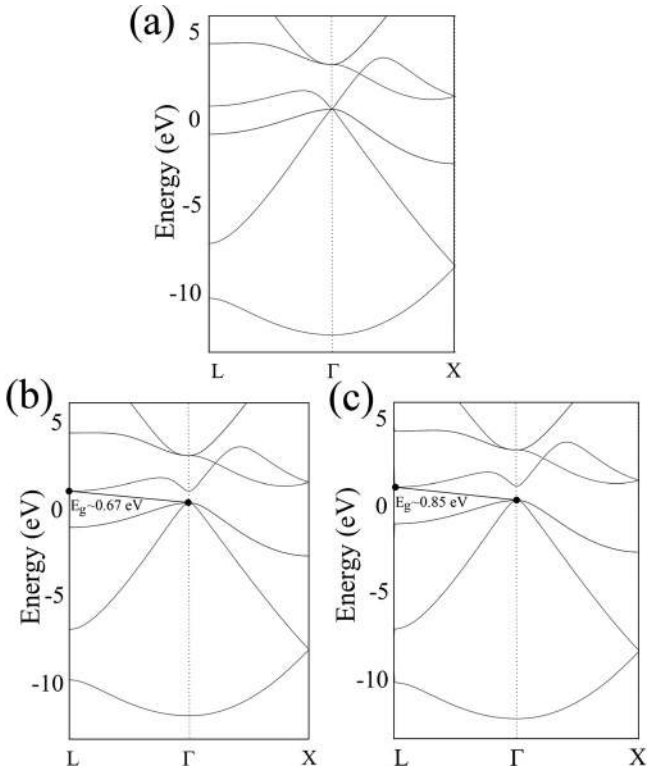

FIG. 6. The band structure of Ge as calculated by Tahini *et al.*[49] using (a) the GGA, (b) the GGA+U, and (c) the HSE06 approaches.

Tahini *et al.*[49] considered the formation energies of the V and E centers in Ge using the formula[96]

$$\Delta H_{D,q}(\mu_e, \mu_\alpha) = E_{D,q} - E_H + \sum_\alpha n_\alpha \mu_\alpha + q\mu_e, \qquad (12)$$

where μ_e is the Fermi energy, μ_a is the chemical potential of the atoms, $E_{D,q}$ is the total energy of the cell containing the defect D in a charge q embedded in the Ge host lattice, and E_H is the total energy of the perfect Ge cell. n_a represents the number of atoms added or removed to the defective cell. The Fermi energy $\mu_e = E_{VBM} + E_f$, with $0 \le E_f \le E_g$. E_{VBM} is the valence band maximum, and E_g is the bang gap. Introducing defects influences the band structure and shifts the electrostatic potential between the prefect Ge lattice and the Ge lattice containing the defect. This shift is commonly corrected (as in Ref. 49) by using a potential alignment correction method[97] by adding $\Delta E_{p\alpha} = q\ \Delta V_{p\alpha}$, where $\Delta V_{p\alpha}$ is the average electrostatic potential difference between the defective and perfect Ge supercells.

Figure 7 represents the formation energies of the V and E centers with respect to the Fermi energy for various charge states, using the GGA + U approach.[49] Table I reports the calculated transition levels between charged states of the V and E centers. For low Fermi energies all the defects considered here are in the neutral charge state. As the Fermi energy increases, there is a range where the singly negatively charge state prevails. This range in Fermi energy is expanded for PV (0.28 eV to 0.52 eV) and AsV (0.26 eV to 0.47 eV) but rather confined for SbV (0.17 eV to 0.18 eV) and V (0.21 eV to 0.27 eV) (refer to Table I).[49] For higher Fermi energies, all the defects considered here become doubly negatively charged.[49]

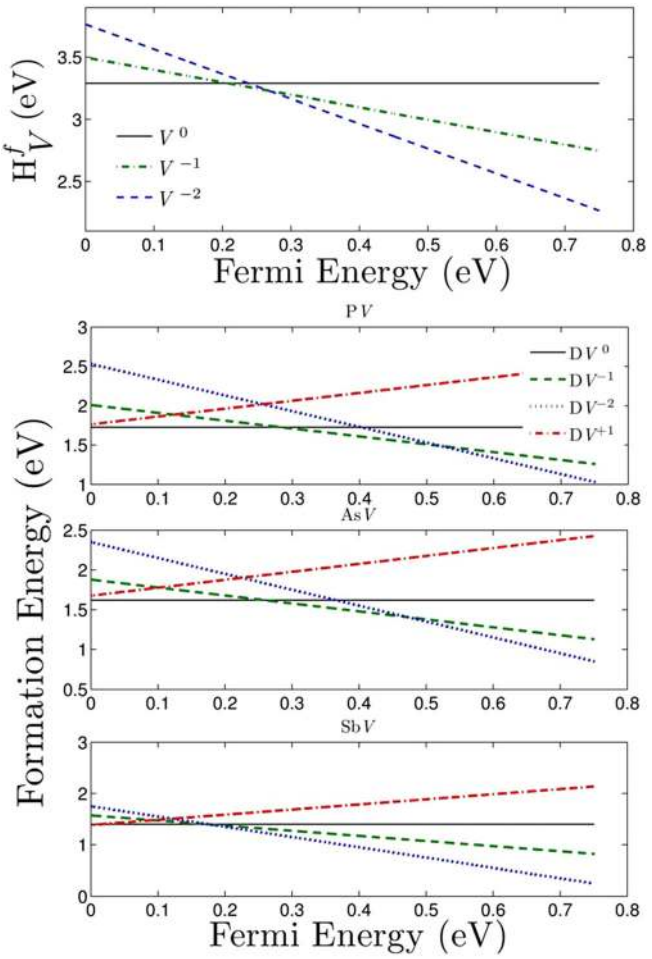

FIG. 7. The formation energies of the V and the E centers, with respect to the Fermi Energy, as calculated using DFT and the GGA+U approach. Reprinted with permission from Tahini *et al.*, Appl. Phys. Lett. **99**, 072112 (2011). Copyright 2011 American Institute of Physics.

The GGA+U investigation of Tahini *et al.*[49] reveals that under n-type doping conditions the PV and AsV can be at -1 or -2 charge states, whereas SbV only at -2 charge state. Experimentally, Brotzmann and Bracht[47] determined that E centers, i.e., AV pairs, in Ge are singly negatively charged under n-type doping conditions. The differences between GGA+U and experiment can be due to the fact that the former is representative at 0 K, whereas the latter for high temperatures. A direct comparison is difficult without information about the impact of temperature on the level position (e.g., entropy effects). However, hybrid DFT may be required to clarify further this issue.

In the V-mediated diffusion mechanism, the donor atom needs to associate with the vacancy. A single exchange in the position between the V and the donor atom does not lead in net diffusion. In the Ge lattice (diamond crystal structure), the V needs to approach the donor atom via a different direction and then exchange position with it in a mechanism known as the ring mechanism of diffusion.[98] Through this process, the donor atom progresses by one lattice site and via the repetition of the process the donor atoms can effectively diffuse (see Fig. 8 for a schematic of the ring mechanism of diffusion). A prerequisite for this type of diffusion mechanisms to take place is that the donor atom must be strongly bound with the vacancy. Otherwise, as the V moves away from the donor atom it will dissociate. In that case the donor atom would be effectively immobilized and require the interaction with another vacancy to migrate further. In the Ge lattice, the V must move away to at least the third-nearest neighbor site (see Fig. 8). The calculated binding energies of E centers are significant and are reported in Table II for the 0 and -1 charge states of the formal and split-vacancy configurations of the AV pair. The formal AV pair consists of a substitutional donor atom and a nearest neighbor vacancy. In the split-vacancy configuration, the donor atom is in-between the Ge lattice sites that are vacant forming semi-vacancies. It has been previously calculated using DFT[37,99] that in the Ge (and Si) lattice, the split-vacancy configuration is energetically favorable for the larger dopants such as Sb, which is larger than Ge. As it can be inferred from Table II, the SbV pair is more energetically favorable by more than -0.1 eV in the split-vacancy configuration as compared to the formal vacancy configuration.[49] Both the PV and AsV pairs are more bound in the formal vacancy configuration and this is expected as P and As are smaller compared to Ge.

Table II also summarizes the most recent DFT[49] migration energies (H_{DV}^m) and activation energies (Q_a) for the E centers in their neutral and negative charge states. The migration energy barriers, H_{AV}^m, effectively quantify the ease with which the AV pairs migrate in the Ge lattice. They are defined here as being the largest relative energy barriers along the ring. Tahini *et al.*[49] used DFT and the nudged elastic band (NEB) method to calculate these barriers for both the neutral and the singly negatively charged AV pairs (see Figure 9).

The activation energy for diffusion, Q_a, is calculated by using the following definition:[37]

$$Q_a = H_V^f + \Delta E_{AV}^1 + H_{AV}^m, \tag{13}$$

where H_V^f is the formation enthalpy of an isolated V and ΔE_{AV}^1 is the binding enthalpy of the AV pair. The calculated activation energies of the singly negatively charged AV pairs are in excellent agreement with the experimental values and values are within 0.11 eV[47,49] (see Table II). Importantly, the DFT and experimental results are consistent with the trend that Q_a decreases with increasing A atom size (although for DFT the $(AsV)^-$ and $(SbV)^-$ have small energy differences).[47,49]

TABLE I. Calculated transition levels between charged states for the V and E centers (eV) using GGA+U.[49]

	PV	AsV	SbV	V
ε(0/-)	0.28	0.26	0.17	0.21
ε(0/--)	0.40	0.37	0.17	0.24
ε(+/-)	0.12	0.10	0.09	…
ε(+/--)	0.26	0.23	0.12	…
ε(-/--)	0.52	0.47	0.18	0.27

E. Insights from DFT on donor deactivation

The maximum dopant solubility in Ge has been studied for more than 50 years.[1,100–102] The maximum solubility of

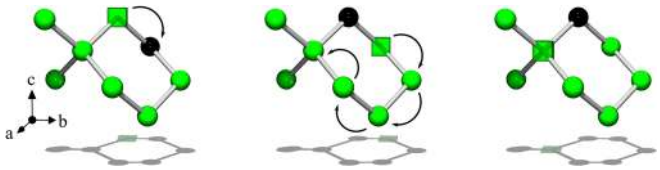

FIG. 8. A schematic representation of the ring mechanism of diffusion in the Ge lattice.

P, As, and Sb is about $6\times 10^{20}\,\mathrm{cm}^{-3}$, $2\times 10^{20}\,\mathrm{cm}^{-3}$, and $1.5\times 10^{20}\,\mathrm{cm}^{-3}$.[100] At high dopant concentration (exceeding $10^{20}\,\mathrm{cm}^{-3}$), the clustering of dopant atoms to form A_nV clusters can lead to the reduction of the activation degree of the implanted dopants.[100,103] In shallow ion implantations, it is common to exceed the solubility limit, and this can lead to dopant precipitation near the peak concentration during thermal annealing processes.[8,100] This is, e.g., revealed as a dopant concentration "spike" in SIMS profiles (see Fig. 10).[8,100,104]

To resolve the nature of the dopant-vacancy clusters in Ge, it is necessary to consider their energetics at the atomistic level. DFT calculations were used to investigate the structures and relative energies of defect clusters formed between dopant atoms and vacancies in Ge.[37,103] As a model system, arsenic-doped Ge was considered.[103] It was calculated that it is energetically favourable to form arsenic-vacancy clusters containing up to four arsenic atoms tetrahedrally coordinated around a vacancy (see Figure 11).[103] DFT calculations consider the energetics of defects at 0 K. As it is important to understand the behavior of clustering at temperatures used during the processing of Ge, mass action analysis was employed.[103] In the mass action analysis framework,[105] the concentration of an As_nV cluster, $[As_nV]$ relative to the unbound As concentration, [As], and the unbound vacancy concentration, [V] is

$$\frac{[As_nV]}{[As]^n[V]}=\exp\left(\frac{-E_b(As_nV)}{k_BT}\right), \tag{14}$$

where k_B is Boltzmann's constant and T is the temperature. In this mass action analysis, changes to the vibrational entropy of the system are assumed to be small and are not included.[105]

Figure 12 represents the temperature dependence of the As concentration assuming an initial As concentration of $10^{19}\,\mathrm{cm}^{-3}$ and an initial vacancy concentration of $10^{18}\,\mathrm{cm}^{-3}$. The As concentration is below the maximum solubility of As in Ge,[1] whereas the vacancy concentration is consistent with the non-equilibrium concentration of vacancies introduced during ion implantation. It is clear from Fig. 12 that at low temperatures, the As_4V cluster (refer to Figure 11) is dominant over unbound vacancies. At higher temperatures, the As_4V cluster dissociates, forming smaller cluster and unbound vacancies.[103] Analogous calculations reveal that for P_4V and Sb_4V clusters, in heavily doped P- and Sb-doped Ge, respectively, the picture is very similar.[37] The mass

TABLE II. Calculated DFT (GGA+U)[49] binding enthalpies (for the formal ΔE^1_{AV} and split-V $\Delta E^1_{A-splitV}$ configurations), migration enthalpies (H^m_{AV}), and activation enthalpies (Q_a) for the E centers (in eV) in their neutral and negative charge states. For comparison, experimental Q_a from SIMS analyses are given in parentheses.[47]

	ΔE^1_{AV}		$\Delta E^1_{A-splitV}$		H^m_{AV}		Q^a	
Defect complex	(-)	(0)	(-)	(0)	(-)	(0)	(-)	(0)
PV	−0.54	−1.57	0.38	−0.47	0.91	1.08	2.79 (2.85)	2.80
AsV	−0.74	−1.68	−0.30	−1.08	0.99	0.95	2.67 (2.71)	2.56
SbV	−0.81	−1.89	−0.93	−2.01	1.17	1.14	2.66 (2.55)	2.42

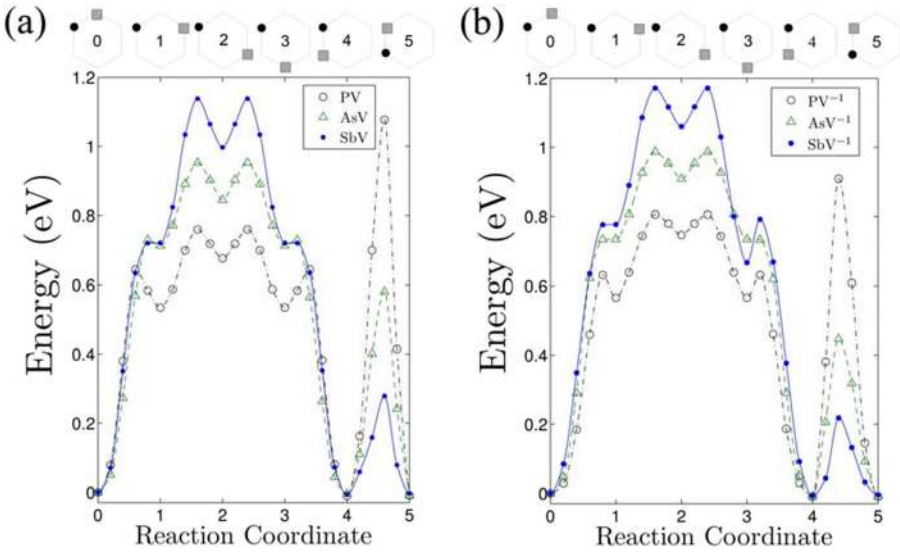

FIG. 9. The migration energy profile of the (a) the neutral and (b) the singly negatively charged AV pairs calculated using DFT (nudged elastic band).[49] On the top is the ring mechanism of diffusion for the DV pair (A = black circles and V = squares) projected onto the (111) surface of Ge.

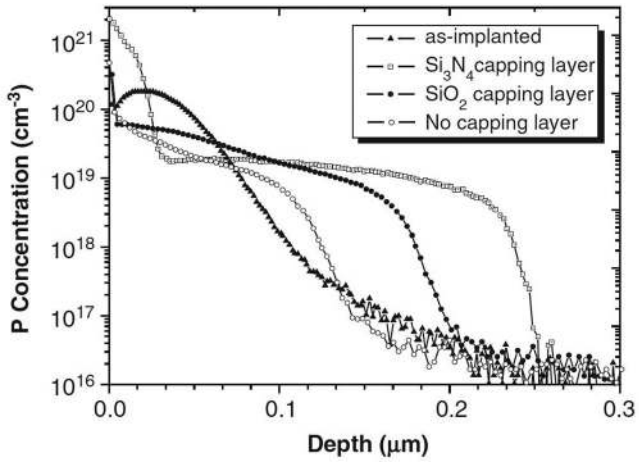

FIG. 10. The phosphorous profiles for uncapped and capped (capping layers SiO_2 and Si_3N_4) after annealing at 500 °C for 2 h implanted Ge samples (P dose: 10^{15} cm^{-2}, implantation energy 30 keV). The as-implanted profile is given for comparison Reprinted with permission from Chroneos *et al.*, Mater. Sci. Semicond. Process. **9**, 640 (2006). Copyright 2006 Elsevier.

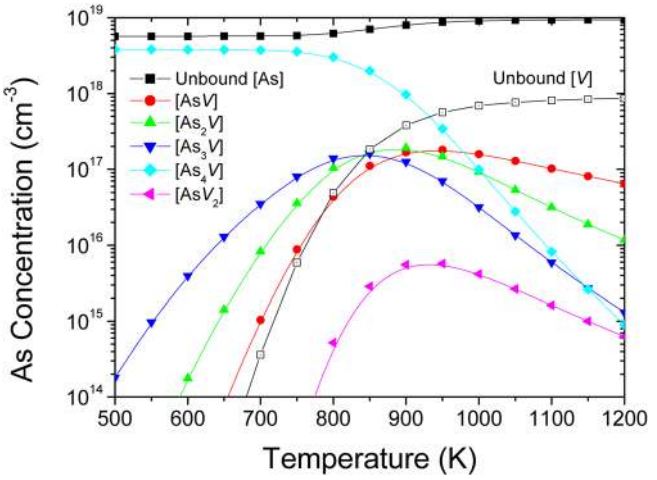

FIG. 12. The temperature dependence of the As concentration of: unbound As atoms, and bound As atoms (bound in As_nV and AsV_2 clusters). The initial As concentration is 10^{19} cm^{-3}, and the initial vacancy concentration is 10^{18} cm^{-3} Reprinted with permission from Chroneos *et al.*, Appl. Phys. Lett. **91**, 192106 (2007). Copyright 2007 American Institute of Physics.

action framework does not consider the kinetics of the processes. These must be investigated in more detail as it may be that the formation of the large As_4V clusters is kinetically hindered. In such a case, the smaller clusters may play a more significant role and may be more populous than predicted by the mass action analysis. Finally, it should be stressed that in Si, previous experimental and theoretical studies attributed to As_nV clusters the electrical deactivation of free carriers in heavily As-doped Si.[106–110] This is an interesting similarity between the two materials, especially when considering that in Si both *V* and *I* impact the defect processes, whereas in Ge vacancies dominate.

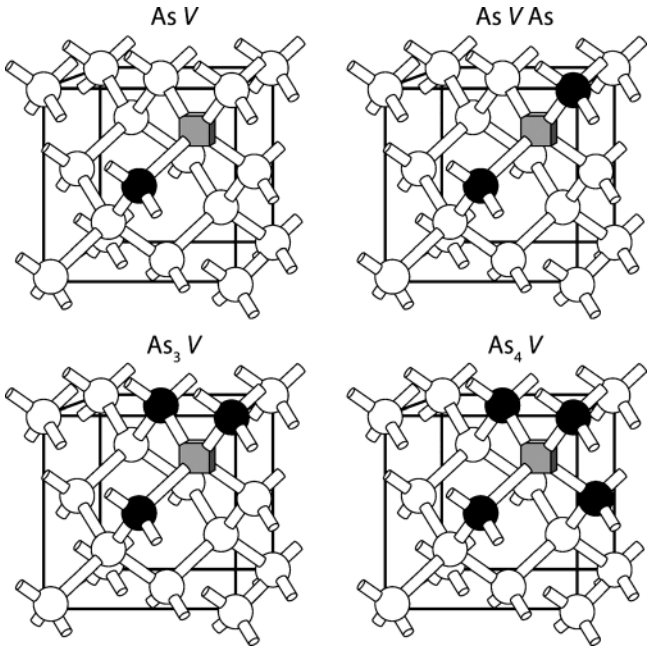

FIG. 11. The highest binding energy As_nV clusters in a unit cell of Ge. Black and white circles represent the As and Ge atoms, respectively, whereas cubes the vacancies Reprinted with permission from Chroneos *et al.*, Appl. Phys. Lett. **91**, 192106 (2007). Copyright 2007 American Institute of Physics.

IV. POINT DEFECT ENGINEERING STRATEGIES TO RESTRAIN DIFFUSION

As already discussed in Sec. III B, dopant diffusion and activation in Ge can be reduced and maximized, respectively, by proper engineering the thermal processing of the implanted Ge. Beside this concept, codoping defect engineering strategies have been proposed to limit the diffusion and clustering of *n*-type dopants.[2,111–114] This is motivated by the fact that defect processes and dopant diffusion in group IV semiconductors can be influenced not only by intrinsic point defects (i.e., vacancies and self-interstitials) but also by codopants.[115–118] The three main codoping strategies propose the use of isovalent codopants (i.e., C, Sn, and Hf), double donor doping (P+As or P+Sb), and fluorine codoping.

A. Isovalent codoping with carbon

The first codopant proposed to limit the diffusion of donor atoms in Ge is carbon.[36,48] Carbon can be introduced in Ge and Si during the Czochralski growth process.[1,119,120] The solubility of carbon in Ge is small as compared to Si;[121] however, it can be introduced in Ge by epitaxial deposition techniques to concentration several orders of magnitude higher than its solubility limit.[93] Carbon is isovalent with Ge and is incorporated at substitutional sites.[1,36] Although in Si the impact of carbon on its defect processes is well established there are relatively few studies in Ge.[122–125] Interestingly, in Si codoping P and C lead to the suppression of the diffusion of P.[124] Regarding the impact of carbon on the diffusion of donor atoms in Ge, this was clarified by diffusion experiment[36] and DFT studies.[48] In particular, in an experimental diffusion study, Brotzmann *et al.*[36] determined that codoping with carbon leads to a reduction of the diffusivity of the donor atoms (P, As, and Sb) (see Fig. 5). In a concurrent DFT study, it was calculated that the introduction of carbon leads to A*V*C clusters and these diffuse with higher migration energies.[48] Additionally, using mass action

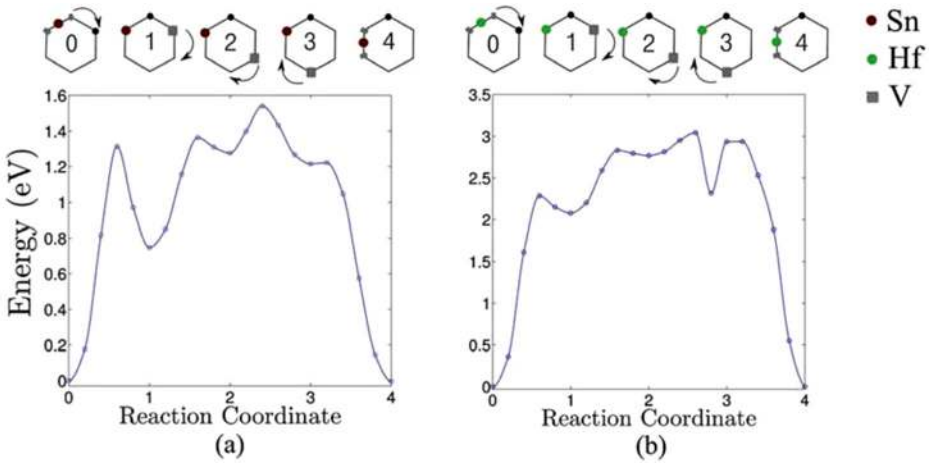

FIG. 13. The diffusion path of PV pairs in the presence of (a) Sn and (b) Hf codopants. The top of the figure represents the ring mechanism of diffusion of the (PSnV)$^{-1}$ and (PHfV)$^{-1}$ clusters Reprinted with permission from Tahini *et al.*, Phys. Chem. Chem. Phys. **15**, 367 (2013). Copyright 2013 Royal Society of Chemistry.

analysis,[105] the concentration of $C_mA_nV_x$ clusters, $[C_mA_nV_x]$, relative to the unbound [C], [D], and [V] is

$$\frac{[C_mA_nV_x]}{[C]^m[A]^n[V]^x} = \exp\left(\frac{-E_b(C_mA_nV_x)}{k_BT}\right). \quad (15)$$

The mass action analysis revealed that a significant proportion of the donor atoms is trapped in C(AV)$_n$ clusters especially when the initial carbon concentration is high (for example, 10^{20} cm^{-3}) and the temperature is low. It is anticipated that the high fraction of these immobile clusters leads to the deactivation of the donor atom profile. This is consistent with the experimental study of Brotzmann *et al.*,[36] which determined that codoping with carbon does not only retard donor diffusion but also reduces the activation inferring that $C_mA_nV_x$ clusters form. Detailed studies on the mechanism of deactivation through clustering will need to be performed.

To conclude, the two main insights of the DFT investigations were that: (a) C traps AV pairs, which will not be able to diffuse further unless they break free of the C atom and (b) for high C-concentrations and low temperatures, a significant proportion of the donor atoms will be trapped in C(AV)$_n$ clusters, leading to deactivation.[48] The DFT predictions are consistent with the experimental results,[36] concluding that although codoping P, As, Sb with C retards their diffusion the deactivation problem remains.[36,48]

B. Codoping with large isovalent atoms

By reducing the concentration of vacancies that are free to associate with donor atoms it is possible to reduce their diffusivity (as V are the vehicle for donor atom diffusion) and deactivation (as V are the key component in the deactivating clusters binding dopants/codopants together). A way to limit the free vacancy concentration is by the association with large isovalent codopants. It is established that oversized atoms such as Sn or Pb can impact the defect processes in group IV semiconductors.[126–128] For example, in recent experimental and DFT studies, it was shown that Sn doping can impact the diffusion and formation of VO pairs (known as A-centers[129]) in Si.[118] The A-center is effectively an oxygen atom at a site near a V.[129] The introduction of the Sn atoms leads to the formation of SnVO clusters, which are very bound and less mobile than the VO in Si.[118]

The E center in Ge is an analogous defect as its key component is also the V (this time associating with a donor atom rather than on O). The introduction of an oversized isovalent substitutional atom leads to local strains in the lattice. The association of the oversized atom with the V is due to the relaxation of these strains as the oversized atom takes advantage of the vacant space. Oversized impurities will typically reside in the space between the semi-vacant lattice sites (split-vacancy configuration).[99,130,131] This association of the codopant isovalent atom with the AV pair leads to high binding energies and effectively influences the migration of the donor atom.[130] Tahini *et al.*[130] investigated using GGA+U the migration of singly negatively charged clusters of (PSnV)$^{-1}$ and (PHfV)$^{-1}$. Figure 13 represents the energies along the path defined at the top of the figure. The migration energy of the (PSnV)$^{-1}$ and (PHfV)$^{-1}$ clusters is 1.54 eV and 3.04 eV, respectively.[130] Comparing this to the migration energy barrier of the (PV)$^{-1}$ (0.91 eV, Table II) or the SnV (1.47 eV, Ref. 131), it is evident that the formation of the (PSnV)$^{-1}$ and (PHfV)$^{-1}$ clusters leads to a significant increase of the migration energies.[130]

Sn codoping with P is promising as the strain compensation (P is smaller and Sn larger than Ge) will increase the solubility of the codopants. This in turn is bound to lead to the increase in the free electron concentration.[100] At any rate, the possibility of formation of larger clusters involving donor, atoms, vacancies, and oversized isovalent atoms needs to be investigated systematically.

C. Double donor atom doping

Doping with P will lead to a contraction of the Ge lattice (P occupies substitutional sites), whereas doping with Sb an expansion. These in turn lead to localized stresses in the vicinity of the dopant reducing the solubility.[100] Codoping P and Sb at an appropriate ratio can lead to the reduction of the dopant related stresses increasing the substitutional solubility of both dopants.[132,133] Kim *et al.*[133] used P+Sb codoping to achieve enhanced n-type dopant activation and reduced implantation damage after rapid thermal annealing.

Tahini *et al.*[134] using a GGA+U approach quantified the binding of P and Sb to the vacancies and the impact of this association to the migration energy of the (PV)$^{-1}$ pairs. To

consider the trapping of the $(PV)^{-1}$ pair to further P or Sb donor atoms, the following reactions were proposed:[134]

$$\begin{aligned}(PV)^{-1} + P_s^+ &\leftrightarrow P_2V,\\ (PV)^{-1} + Sb_s^+ &\leftrightarrow PSbV.\end{aligned} \tag{16}$$

The binding energies of the P_2V and PSbV clusters are calculated to be −1.83 eV and −2.03 eV, respectively.[134] This difference of −0.2 eV in the binding energies can be attributed to the relaxation of the Sb atom near the vacant space of the PV pair in agreement with the arguments of Kim *et al.*[133] Tahini *et al.*[134] concluded that the formation of the PSbV clusters reduces the concentration of the highly mobile $(PV)^{-1}$ pairs. Additionally, the migration energy of the PSbV clusters is more than 1 eV higher as compared to the $(PV)^{-1}$ pairs.[134] In essence the Sb atoms will trap and immobilize the PV pairs.

Double-donor doping with P+AS was also proposed as a way to increase the active donor concentrations.[111] DFT calculations in conjunction with mass action analysis concluded that P+As doping is a way to engineer the active donor concentrations.[111] This inspired the experimental work of Tsouroutas *et al.*,[16] which concluded that although there is a retardation of the As diffusion (note P has a higher activation energy of diffusion than As[46,48]), the activation level of the P+As samples is typically lower compared to the singly doped samples.

D. Codoping with fluorine

The ideal codopant to a donor atom should interact strongly with the vacancy but not the donor atom as the latter atom may lead in A-V-codopant cluster formation and in turn deactivation. Fluorine is a candidate codopant due to its very high electronegativity. Numerous previous studies[135–143] investigated the impact of F doping and codoping in Si with F providing evidence on the formation of F_nV_m clusters. Experimental work[136] on F-implanted preamorphized Si determined that the formation of F_nV_m clusters is detected. At any rate, the community agrees that F implantation effectively suppress the transient-enhanced self-interstitial mediated diffusion of acceptor atoms such as B in Si.[136,140]

DFT calculations indicate that when fluorine is introduced in Ge, it forms very bound F_nV_m clusters.[112] To understand the structure of these clusters, one has to consider their formation at an atomistic level. The first defect to consider is the F interstitial, which forms in-between two Ge atoms in a bond-center position. The F interstitial forms two covalent bonds and releases an electron (F becomes positively charged) to the crystal.[140] In the tetrahedral position, the F interstitial captures an electron to complete its outer shell and is therefore expected to be negatively charged.[112] In Ge, DFT calculations reveal that bond-center configuration is energetically favourable as compared to the tetrahedral configuration by 0.38 eV.[112] This is consistent to Si, where again the bond-center configuration is prevalent.[139,140] The F_2 interstitial pair consists of a bond-center and a tetrahedral interstitial, which are oppositively charged and attract each other with a binding energy of −0.97 eV.[112] The positively charged bond-center F interstitials attract the doubly negatively charged V (dominant in Ge under intrinsic and n-type doping conditions, Fig. 7 and Ref. 49) forming the F_nV_m clusters.[112] It should be noted that for every V, there exist four dangling bonds. As an F interstitial encounters a dangling bond, the bond is saturated by forming a FV pair (binding energy of −1.19 eV, F–Ge bond distance 1.8 Å).[112] In F_nV_m clusters, F interstitials are attracted to the V forming stable clusters until all four dangling bonds per vacancy are saturated. DFT calculations reveal that in the most stable cluster configurations, the F atoms are displaced from in-line V–F–Ge dangling bond directions so that they allow for the F atoms to be more separated.[112] For all the F_nV_m clusters considered the DFT calculations revealed that the energy gain for every F interstitial added is more than 1 eV.[112] Another finding is that clusters in which all dangling bonds are saturated exhibit the highest binding energies.

In F-doped Ge, mass action analysis was used to quantify the relative concentrations of F_nV_m clusters, relative to the concentration of unbound F atoms, [F], and unbound V

$$\frac{[F_nV_m]}{[F]^n[V]^m} = \exp\left(\frac{-E_b(F_nV_m)}{k_BT}\right). \tag{17}$$

It is clear from Eq. (17) that the formation of the larger clusters is strongly dependent upon the [F] and [V]. To illustrate this point, Figure 14 represents the temperature dependence of the concentration of F_nV_m clusters for (a) F concentration of $10^{17}\,cm^{-3}$ and (b) F concentration of $10^{18}\,cm^{-3}$ assuming in both cases an initial vacancy concentration of $10^{18}\,cm^{-3}$.[112] In essence, two sets of simultaneous equations for F_nV_m clusters were considered and solved separately using an iterative minimization approach.[112]

At temperatures below 865 K, most of the V that participate in clusters form V_4 clusters (Fig. 14(a)). The V_4 clusters' concentration falls as temperature rises and at the temperature range of 865–1005 K, the F_2V_2 becomes the dominant cluster. Notably, most V remains as isolated species. The increase of the temperature leads to the dissociation of the F_2V_2 clusters and the increase in the concentration of the FV pairs, which can be mobile.[112] All the other clusters are insignificant from a concentration point of view as they never trap more than 2% of V in the temperature range considered.[112]

Increasing the implanted F concentration to equal the V concentration changes significantly the results (compare Figs. 14(a) and 14(b)). As it can be deduced from Fig. 14(b) up to 1165 K, the F_3V_2 cluster and the F_2V_2 account for most of the trapped V concentration (for example, at 850 K, these two clusters trap about 70% of V).[112] Above 1165 K, the concentration of FV pairs increase so that they trap more V than any other cluster. Another interesting feature that appears in Fig. 14(b) is that the larger electrically inactive clusters for which all dangling bonds are saturated (such as F_4V and F_2V_6) appear, but they are of limited concentration. This is also the case for all other clusters considered (such as the F_5V_2, F_4V_2, and FV_2) that only trap a few percent of the total vacancy concentration.[112] Mass action analysis reveals that codoping with F at concentrations of $10^{18}\,cm^{-3}$ (or higher than the V concentration) is sufficient for trapping the V.

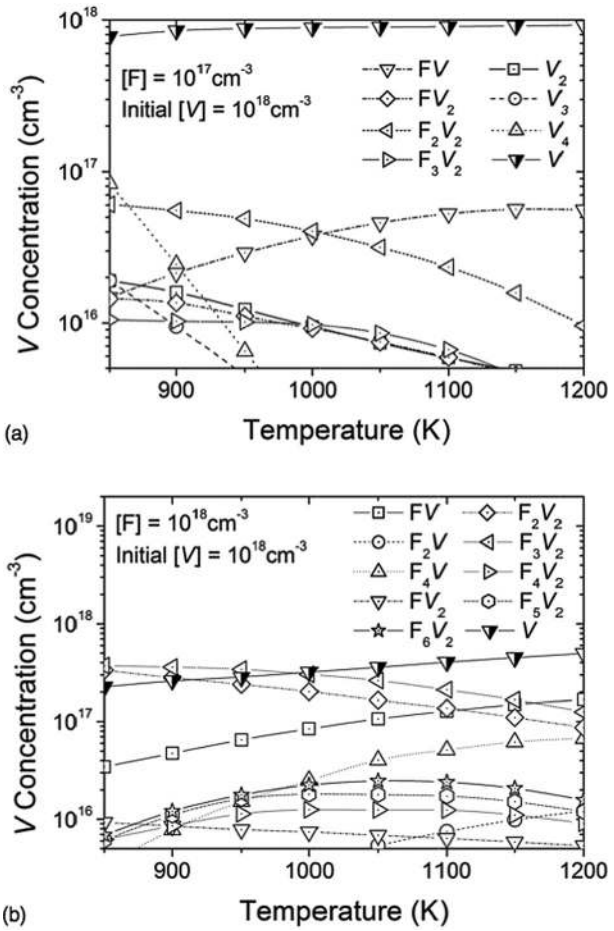

FIG. 14. The temperature dependence of the concentration of F_nV_m clusters for (a) F concentration of $10^{17}\,cm^{-3}$ and (b) F concentration of $10^{18}\,cm^{-3}$. The initial vacancy concentration is $10^{18}\,cm^{-3}$ Reprinted with permission from Chroneos *et al.*, J. Appl. Phys. **106**, 063707 (2009). Copyright 2013 American Institute of Physics.

Figure 14 reports results of F-doped Ge; however, to fully comprehend the impact of F on P*V* pairs and more extended P-vacancy clusters, one needs to consider the formation of these clusters in P-doped Ge (refer to Fig. 15(a)) and P/F codoped Ge (refer to Fig. 15(b)). Figure 15(a) represents the temperature dependence of the concentration of P related clusters as well as unbound P atoms and unbound *V* (here, $[V] = 10^{18}\,cm^{-3}$ and $[P] = 10^{19}\,cm^{-3}$).[112] Analogously to As-doped Ge (refer to Sec. III C) at lower temperatures, the P_4V clusters are dominant in concentration; however, with the increase in temperature, they break up into smaller P_nV clusters and isolated defects. The P*V* pairs become dominant concentration-wise at around 850 K; however, at this temperature, most of the P atoms are isolated (Fig. 15(a)).[112] With a further increase in the temperature, the remaining P_nV clusters dissociate further (Fig. 15(a)).[112]

Codoping P with F aims to overcome the technological problem caused by the mobile P*V* pairs that lead to the formation of less sharp doped regions. In essence, it is anticipated that the introduction of F will lead to the formation of F_nV_m clusters in preference to P*V* pairs. In essence the formation of F_nV_m clusters will reduce the concentration of free *V* and through defect equilibria also the concentration of P*V* pairs. As the diffusion of P in Ge requires the formation of P*V* pairs this will effectively lead to the reduction of P diffusivity. Figure 15(b) represents the mass action results for P and F codoping assuming an initial *V* concentration of $10^{18}\,cm^{-3}$, F concentration of $10^{18}\,cm^{-3}$, and P concentration of $10^{19}\,cm^{-3}$.[112] P and F codoping leads to the reduction in the deactivating P_nV clusters and the mobile P*V* pairs (refer to Figs. 15(a) and 15(b)). Most of the *V* are effectively trapped in F_2V_2 and F_3V_2 clusters, whereas the clusters containing P and V are not important concentration-wise[112] Previous studies observed an analogous behavior for As and F codoping.[112]

The key result of the DFT/mass action analysis study[112] is that codoping an *n*-type dopant (such as P or As) with fluorine leads to the formation of F_nV_m clusters reducing the vacancy concentration available to interact with P (or As). This in turn leads to the practical demise of both the diffusion of donor atoms (P*V* pairs are required) and the deactivating clusters.[112]

In a subsequent experimental and DFT study, Impellizzeri *et al.*[2] support the viewpoint that F is an appropriate codopant for As. This investigation determined that

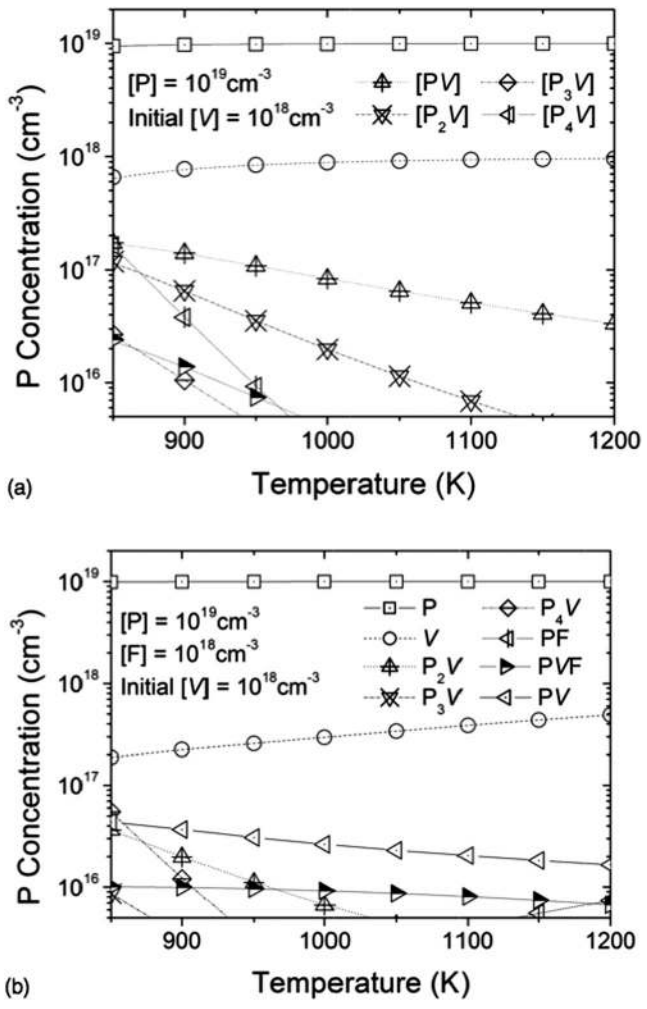

FIG. 15. The temperature dependence of the P concentration (of unbound P atoms, and bound P atoms) and unbound *V* for (a) P-doped Ge and (b) P and F codoped Ge. The initial P concentration is $10^{19}\,cm^{-3}$, F concentration of $10^{18}\,cm^{-3}$, the initial vacancy concentration is $10^{18}\,cm^{-3}$ Reprinted with permission from Chroneos *et al.*, J. Appl. Phys. **106**, 063707 (2009). Copyright 2013 American Institute of Physics.

the implantation with F creates a supersaturation of V, which in turn enhances the diffusion of As in the layer that is amorphized by F and As implantation.[2] This layer is subsequently regrown by solid phase epitaxy and the clusters consisting of F atoms and Ge interstitials form near the end of range damaged region.[2] These clusters act as sinks for the vacancies and/or sources of self-interstitials and importantly lead to the suppression of both As diffusion and the formation of deactivating arsenic-related clusters.[2] This in essence proves that F codoping the way to achieve better and simultaneous control of n-type dopant diffusion and activation during germanium device processing.[2,112]

The spreading resistance profiling study of Jung *et al.*[144] determined that vacancies in Ge are acceptors and anneal out near 600 °C. Implanted F atoms passivate the V (at around 500 °C), leading to a potential enhancement in Ge-MOSFET performance.[144] The DFT and experimental evidence consistently show that codoping donor atoms with F is an efficient way to annihilate vacancies and improve Ge-devices.[2,112,144]

V. INTERSTITIAL MEDIATED DIFFUSION UNDER PROTON IRRADIATION

Efficient defect engineering strategies that aim to control the diffusion and activation of dopants in Ge must control the concentration and distribution of both V and I and also the balance between these intrinsic defects. Ion implantation is known to create both V and I. Post-implantation annealing leads to the removal of the implantation damage or the evolution of microscopic defects depending on the temperature applied. The defect reactions occurring during post-implantation annealing are quite complex and hardly understood in full detail. Generally, it is difficult to gain reliable information about the defects and their interactions under non-equilibrium experiments.

However, defined non-equilibrium conditions can be realized by concurrent annealing and irradiation with light particles such as electrons or protons. These particles mainly form isolated V and I in equal numbers. The effect of proton irradiation on self- and dopant diffusion in Ge was recently studied by means of isotopically controlled Ge and natural Ge samples doped with P, As, and B.[72,145,146] Analysis of self- and dopant diffusion in Ge under irradiation revealed a surprising diffusion behavior. This is demonstrated by Figs. 16–18 that indicate experimental results on self-diffusion, boron diffusion, and arsenic diffusion under concurrent annealing and irradiation. Whereas the diffusion of self- and B-atoms is clearly enhanced compared to thermal equilibrium conditions, the diffusion of n-type dopants such as P and As remains unaffected, i.e., equals the diffusion under thermal equilibrium conditions.[72,145,146] In Ref. 145, a retarded diffusion of P under irradiation is reported, which is at variance with the results presented in this work and more recently in Ref. 146. The seemingly retarded diffusion of P under irradiation in Ref. 145 is suggested by an enhanced outdiffusion of P to the sample surface. This outdiffusion was not sufficiently suppressed by a SiO_2 layer deposited on the Ge surface and lead to a P dose loss of about 70% of the total P-implanted dose. Experiments with P-implanted samples capped with silicon nitride and As-implanted samples capped with SiO_2 do not reveal a retarded diffusion under irradiation.[146] Nonetheless, donor diffusion in Ge under irradiation behaves unusual as it fully resembles donor diffusion under thermal equilibrium conditions, that is, an enhancement of donor diffusion due to irradiation is not

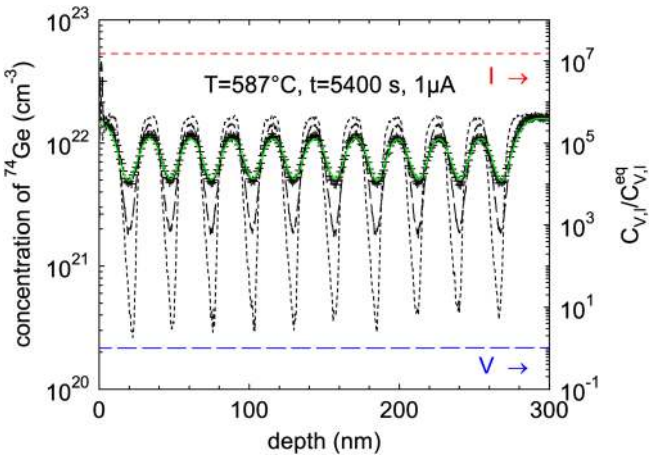

FIG. 16. Concentration profile of ^{74}Ge (+) measured with secondary ion mass spectrometry after annealing a (^{nat}Ge/^{70}Ge)$_{10}$ isotope multilayer structure at 587 °C for 5400 s and concurrent irradiation with 2.5 MeV protons at a flux of 1 μA. The green solid line represents the best fit to the experimental ^{74}Ge profile based on the model for Ge self-diffusion under irradiation proposed by Schneider *et al.*[72] The calculated concentrations of V and I normalized to their thermal equilibrium values are referred to the right axis. The distributions of both V and I are homogeneous with V concentrations close to thermal equilibrium and I concentrations in high supersaturation. The short-dashed profile reflects the ^{74}Ge profiles of the as-grown isotope structures. The long-dashed line represents the Ge profile beneath a covered part of the Ge sample. This part was not irradiated and, accordingly, shows self-diffusion under thermal equilibrium conditions.

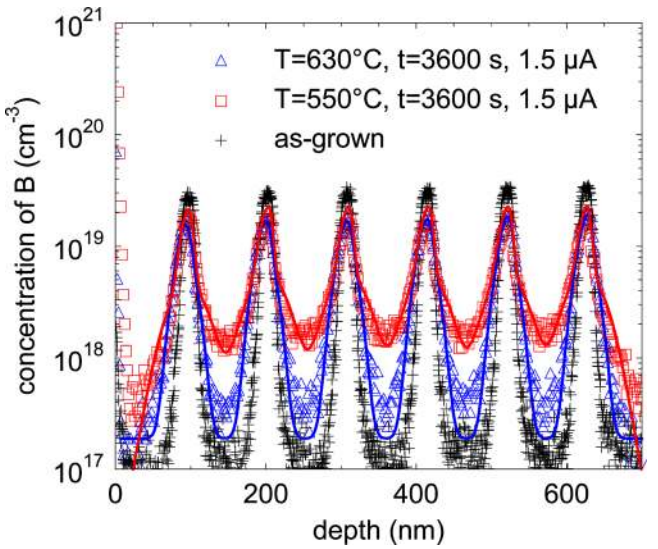

FIG. 17. Concentration profiles of boron (B) in Ge measured with secondary ion mass spectrometry after concurrent annealing and irradiation with 2.5 MeV protons (Δ, □) and experimental conditions as indicated in the figure. The distribution of B in the as-grown structure (+) is shown for comparison. The B profiles reveal a stronger diffusional broadening at low compared to high temperatures. The solid lines are theoretical B profiles calculated on the basis of the B diffusion model described by Schneider *et al.*[72] The model considers contributions of substitutional B_s, BI pairs, and immobile B clusters to the total B concentration.

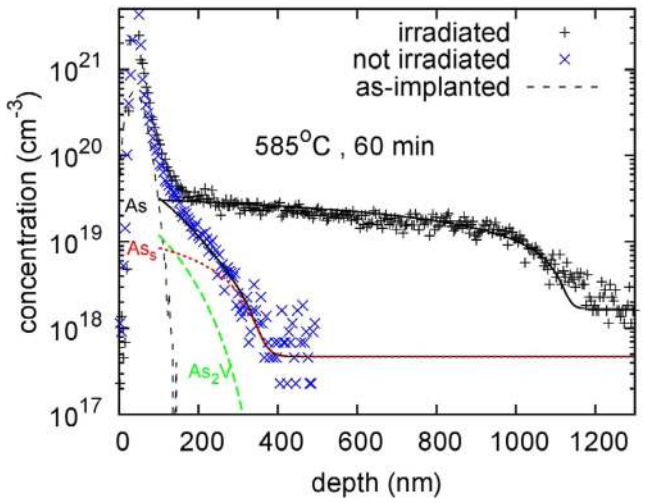

FIG. 18. Concentration profiles of arsenic (As) in Ge measured with secondary ion mass spectrometry after As implantation (thin black dashed line) and additional annealing (symbols) at the temperature and time indicated. The diffusion behavior of As under irradiation (+) and non-irradiation (×) is very different as demonstrated by the differences in profile shape and penetration depth. Arsenic diffusion is accurately described on the basis of reactions (8), (10), and (18). The position of the amorphous/crystalline (a/c) interface formed by As implantation at about 100 nm from the surface is taken as onset of the diffusion profile. Arsenic within about 100 nm from the surface likely exists in clusters that are more complex than As_2V. These clusters are considered to dissolve during annealing and serve as constant source for dopant diffusion. Below the a/c-interface the As profile after concurrent annealing and irradiation (+) is accurately described by the vacancy mechanism (8) with full activation of the dopant that reflects the contribution of reaction (18). The dopant profile after annealing without irradiation reveals the formation of dopant-vacancy A_2V complexes and a corresponding lower level of activation. The profiles of the electrical active substitutional As_s and inactive As_2V complexes deduced from the simulation of As diffusion without irradiation are indicated by the red and green dashed lines, respectively.

evident. In addition, self- and B diffusion does not reveal any depth dependence that is expected in the case the Ge surface acts as efficient sink for native defects (see Figs. 16 and 17). The behavior of self- and dopant diffusion in Ge under irradiation strongly differs from that in Si[147] and, accordingly, must be due to properties of Ge that strongly differ from Si. First, the equilibrium diffusion of As and P under irradiation demonstrates that the concentration of V in Ge under irradiation does not significantly deviate from thermal equilibrium.[146] Second, the absence of any depth-dependent broadening in self- and dopant diffusion shows that the distribution of the native defects must be homogeneous.[72] Third, the enhanced diffusion of B under irradiation indicates that B diffusion must be mainly mediated by I, whose concentration exceeds the thermal equilibrium value by several orders of magnitude.[72] The characteristic behavior of self- and dopant diffusion in Ge under concurrent annealing and irradiation is explained consistently only with a Ge surface that acts as efficient sink for V but as barrier for I. As a consequence, a strong imbalance between I and V is built up during irradiation with homogeneous distributions but V concentrations close to thermal equilibrium and I concentrations exceeding thermal equilibrium by several orders of magnitude.[72,146]

The apparent equilibrium diffusion of P and As in Ge under irradiation is a quite unusual behavior. This shows that the concentration of V is in thermal equilibrium even under irradiation and that donor diffusion via dopant-I pairs is not favorable even under I-supersaturation. The imbalance between the V and I concentration is due to the disparity of the surface to annihilate V and I. The negligible diffusion via dopant-I pairs is explained by Coulomb repulsion between the donor and I[148] since both defects are positively charged.

It is noted that the diffusion of donors in Ge under irradiation resemble equilibrium diffusion although a I-supersaturation exists. This shows that for dopant diffusion via the vacancy mechanism (8) the concentrations of V and AV pairs matters. As long as vacancies are in thermal equilibrium also the concentration of AV pairs does not deviate from equilibrium and donor diffusion remains unaffected. Hence, the question rises what is the difference between donor diffusion under thermal equilibrium and non-equilibrium conditions the latter being established by concurrent annealing and irradiation? The striking difference is that concurrent annealing and irradiation suppresses the deactivation of donors.[146] At first sight, one could expect that this is due to reactions $AV^- + I^{2+} \leftrightarrow A_s^+$ and $A_2V + I^{2+} \leftrightarrow 2A_s^+$ but since equilibrium conditions hold for V under concurrent annealing and irradiation, equilibrium conditions must also hold for AV^- based on reaction (8). The suppressed deactivation of donors implies that reaction (10) cannot be operative under concurrent annealing and irradiation. This behavior is explained by means of a competitive inhibition reaction.[149] Such reactions are known from biochemical enzymatic reactions. In our case, self-interstitials act as inhibitors for the formation of A_2V complexes without forming stable AI pairs. The inhibitor reaction described by

$$\begin{array}{l} A_s^+ + AV^- \leftrightarrow A_2V^0 \\ + \\ I^{2+} \\ \updownarrow \\ AI^{3+} \end{array} \qquad (18)$$

lowers the rate constant for the formation of the A_2V complex. The suppression of A_2V formation increases with increasing I-supersaturation. The inhibitor reaction describes the tendency of the substitutional donor to form a pair with I favored due to long-range elastic interactions. However, the repulsive Coulomb interaction finally hampers the actual formation of the pair.

Key of the interpretation of self- and dopant diffusion in Ge under concurrent annealing and irradiation is the limited efficiency of the Ge surface to annihilate self-interstitials.[148] This unusual behavior is independently supported by the detection of I in Ge by means of high resolution transmission electron microscopy.[150] The identification of I would be hardly possible in the case the Ge surface is a perfect sink.

Self- and dopant diffusion in Ge under concurrent annealing and irradiation conditions demonstrate the significance of I. Unfortunately, information about the properties of I in Ge are very limited as this native defect is not relevant

for diffusion in Ge under thermal equilibrium conditions.[72,87] Recently, Cowern *et al.*[59] used B diffusion measurements to probe the nature of *I* in Ge. They report on two distinct self-interstitial forms, i.e., one form with a low and another with high activation entropy. This was concluded from the analysis of B diffusion based on the g/λ approach.[151] However, the applicability of this approach for the analysis of B diffusion in Ge under non-equilibrium conditions is highly questionable since several assumptions considered in this approach are not fulfilled. A more rigorous analysis of B diffusion in Ge, which is based on the full system of differential diffusion equations,[72] does not confirm the existence of two forms of *I* defects in Ge. Instead, the analysis reveals that the concentration of B*I* pairs formed between B and *I* can strongly exceed the concentration of substitutional B under irradiation. The formation entropy of the B*I* pair was determined to 30 k_B,[72] whereas for the migration entropy of *I*, a value of about 4 k_B was found. Although the total activation entropy, i.e., sum of formation and migration entropy, of the B*I* pair and the isolated *I* are not accessible, the analysis confirms the presence of two distinct forms of *I*s, but the more extended form is a B*I* pair rather than another form of a self-interstitial. This distinction between B*I* and *I* is difficult in the g/λ approach.

Experimental conditions are advantageous for the fabrication of Ge-based electronic devices that suppress the deactivation of donors without enhancing their mobility. However, the increased activation observed under concurrent annealing and irradiation enhances donor diffusion according to its strong doping dependence. To compensate for the enhanced diffusion, the annealing time must be reduced.

Other strategies to alter the diffusion and activation of dopants in Ge rely on the formation and dissolution of defect clusters that, e.g., emit self-interstitials. Self-interstitials are, e.g., injected by Ge oxide nanoclusters (NC) formed in Ge by oxygen implantation and subsequent annealing.[152] Moreover, the dissolution of fluorine-*I* clusters have been demonstrated to retard the diffusion of As.[2] The concept of forming NC that inject *I* either during their formation or dissolution is also well suited to alter the balance between *V* and *I*.

Finally, codoping strategies have been considered to suppress the diffusion and deactivation of donors. These strategies can reduce the free vacancy concentration as supported by the calculations presented in Sec. IV. However, it is important to note that the calculations consider fixed concentration of *V*, i.e., no additional *V* sources are assumed. This condition is hardly fulfilled experimentally as realistic samples possess *V* sources like free surfaces that supply vacancies. Accordingly, although codoping strategies are expected to limit the diffusion of donors, an efficient suppression of the deactivation is unlikely because vacancies trapped by co-dopants are rapidly supplied from free surfaces.

Irrespective of the method used to change the balance between *I* and *V*, i.e., either by concurrent annealing and irradiation or by post-implantation annealing, the Ge surface strongly affects the *I*-*V* balance. Therefore, understanding of the surface property is of fundamental significance to develop successful defect engineering strategies to control the diffusion and activation of dopants in Ge during device fabrication.

VI. SUMMARY AND FUTURE DIRECTIONS

DFT calculations can provide insights that can support and complement advanced experimental studies. Importantly, experimental diffusion studies and DFT are in agreement that donor atom diffusion in Ge is via a vacancy-mechanism. Both approaches are consistent on the underlying trend observed in the activation energy of donor atom diffusion, i.e., with increasing dopant size the activation energy decreases. Additionally, they offer complementary information when considering charge states or the structure and concentration of technological important donor-vacancy clusters. Throughout this review, it was demonstrated how DFT can be utilized to design point defect engineering strategies. Defect engineering strategies to retard donor atom diffusion and deactivation in Ge is a key issue in the realization of *n*-type Ge-MOSFET. Full flexibility in defect engineering strategies requires controlling the formation of both vacancies and self-interstitials and their balance. Moreover, the impact of free surfaces on the *V*-*I* imbalance must be understood in more detail as the Ge surface properties strongly affect defect reactions under non-equilibrium conditions. The present review highlights strategies that may inspire experiments. For example, it was proposed using a DFT/mass action analysis approach that fluorine codoping in germanium can suppress donor diffusion and deactivation.[112] These results have being validated experimentally[2] two years after the publication of the DFT/mass action analysis[112] and have recently led to claims of the improvement in the performance of Ge-MOSFET.[144]

Capping layers on Ge during the activation anneal can influence the out-diffusion of implanted dopants.[8,17] The stresses introduced by the capping layer to the near surface Ge layer may impact the distribution of point defects and the out-diffusion of the dopant atoms. These issues have been investigated using DFT in Si,[153] but a systematic study in Ge should be rewarding as with the dimensions of devices being further scaled down surfaces and interfaces will become increasingly important. In general, the introduction of strain or the consideration of $Sn_{1-x}Ge_x$ (or $Si_{1-x-y}Ge_xSn_y$) alloys are relatively unchartered areas of research.[19,154–158] For example, $Sn_{1-x}Ge_x$ alloys provide a range of strain option, which enables them to be applied as buffer layers to lattice match Si or Ge substrates with most III–V and II–VI compounds.[155,156] The properties on *n*-type dopants in $Sn_{1-x}Ge_x$ and $Si_{1-x-y}Ge_xSn_y$ alloys have not been investigated in detail.

ACKNOWLEDGMENTS

The authors acknowledge discussions over the years with Professor Robin Grimes and Dr. Hassan Tahini (Imperial College London). This work was funded by the Deutsche Forschungsgemeinschaft under Grants BR 1520/6-2 as well as an individual Grant within the Heisenberg program for HB.

[1]C. Claeys and E. Simoen, *Germanium-Based Technologies: From Materials to Devices* (Elsevier, 2007).
[2]G. Impellizzeri, S. Boninelli, F. Priolo, E. Napolitani, C. Spinella, A. Chroneos, and H. Bracht, J. Appl. Phys. **109**, 113527 (2011).

[3]N. A. Stolwijk and H. Bracht, *Diffusion in Silicon, Germanium and their Alloys*, Landolt-Börnstein New Series Vol. III/33, Subvolume A (Springer, New York, 1998); H. Bracht and N. A. Stolwijk, *Solubility in Silicon and Germanium*, Landolt-Börnstein New Series Vol. III/41, Subvolume A2α (Springer, New York, 2002).
[4]H. Bracht and S. Brotzmann, Mater. Sci. Semicond. Process. **9**, 471 (2006); H. H. Silvestri, H. Bracht, J. L. Hansen, A. N. Larsen, and E. E. Haller, Semicond. Sci. Technol. **21**, 758 (2006).
[5]A. Chroneos, R. W. Grimes, and C. Tsamis, Mater. Sci. Semicond. Process. **9**, 536 (2006).
[6]H. M. Pinto, J. Coutinho, V. J. B. Torres, S. Öberg, and P. R. Briddon, Mater. Sci. Semicond. Process. **9**, 498 (2006).
[7]P. Tsouroutas, D. Tsoukalas, A. Florakis, I. Zergioti, A. A. Serafetinides, N. N. Cherkashin, B. Marty, and A. Claverie, Mater. Sci. Semicond. Process. **9**, 644 (2006).
[8]A. Chroneos, D. Skarlatos, C. Tsamis, A. Christofi, D. S. McPhail, and R. Hung, Mater. Sci. Semicond. Process. **9**, 640 (2006); A. Chroneos, Phys. Status Solidi B **244**, 3206 (2007); H. Tahini, A. Chroneos, R. W. Grimes, U. Schwingenschlögl, and A. Dimoulas, J. Phys. Condens. Matter **24**, 195802 (2012).
[9]E. E. Haller, Mater. Sci. Semicond. Process. **9**, 408 (2006).
[10]C. Janke, R. Jones, J. Coutinho, S. Öberg, and P. R. Briddon, Phys. Rev. B **77**, 195210 (2008).
[11]A. Chroneos, H. Bracht, R. W. Grimes, and B. P. Uberuaga, Mater. Sci. Eng., B **154–155**, 72 (2008).
[12]M. Naganawa, Y. Shimizu, M. Uematsu, K. M. Itoh, K. Sawano, Y. Shiraki, and E. E. Haller, Appl. Phys. Lett. **93**, 191905 (2008).
[13]S. Schneider, H. Bracht, M. C. Petersen, J. Lundsgaard Hansen, and A. Nylandsted Larsen, J. Appl. Phys. **103**, 033517 (2008).
[14]E. Hüger, U. Tietze, D. Lott, H. Bracht, D. Bougeard, E. E. Haller, and H. Schmidt, Appl. Phys. Lett. **93**, 162104 (2008).
[15]A. Chroneos, H. Bracht, C. Jiang, B. P. Uberuaga, and R. W. Grimes, Phys. Rev. B **78**, 195201 (2008).
[16]P. Tsouroutas, D. Tsoukalas, and H. Bracht, J. Appl. Phys. **108**, 024903 (2010).
[17]A. Chroneos, J. Appl. Phys. **105**, 056101 (2009).
[18]E. Bruno, S. Mirabella, G. Scapellato, G. Impellizzeri, A. Terrasi, F. Priolo, E. Napolitani, D. De Salvador, M. Mastromatteo, and A. Carnera, Phys. Rev. B **80**, 033204 (2009).
[19]A. Chroneos, C. Jiang, R. W. Grimes, U. Schwingenschlögl, and H. Bracht, Appl. Phys. Lett. **94**, 252104 (2009); J. J. Pullikotil, A. Chroneos, and U. Schwingenschlögl, J. Appl. Phys. **110**, 036105 (2011).
[20]S. Decoster, B. De Vries, U. Wahl, J. G. Correia, and A. Vantomme, J. Appl. Phys. **105**, 083522 (2009).
[21]J. Oh and J. C. Cambell, Mater. Sci. Semicond. Process. **13**, 185 (2010).
[22]M. Werner, H. Mehrer, and H. D. Hochheimer, Phys. Rev. B **32**, 3930 (1985).
[23]A. J. R. da Silva, A. Janotti, A. Fazzio, R. J. Baierle, and R. Mota, Phys. Rev. B **62**, 9903 (2000).
[24]R. A. Logan, Phys. Rev. **101**, 1455 (1956).
[25]A. Giese, N. A. Stolwijk, and H. Bracht, Appl. Phys. Lett. **77**, 642 (2000).
[26]J. Vanhellemont, P. Spiewak, and K. Sueoka, J. Appl. Phys. **101**, 036103 (2007).
[27]H. Bracht and A. Chroneos, J. Appl. Phys. **104**, 076108 (2008).
[28]N. A. Stolwijk and L. Lerner, J. Appl. Phys. **110**, 033526 (2011).
[29]J. A. Van Vechten, Phys. Rev. B **33**, 2674 (1986).
[30]J. Coutinho, R. Jones, P. R. Briddon, and S. Öberg, Phys. Rev. B **62**, 10824 (2000).
[31]A. Chroneos and C. A. Londos, J. Appl. Phys. **107**, 093518 (2010).
[32]A. Chroneos, C. A. Londos, and H. Bracht, Mater. Sci. Eng. B **176**, 453 (2011).
[33]A. Chroneos, R. W. Grimes, and H. Bracht, J. Appl. Phys. **105**, 016102 (2009); A. Chroneos, J. Appl. Phys. **107**, 076102 (2010); A. Chroneos, C. A. Londos, and E. N. Sgourou, J. Appl. Phys. **110**, 093507 (2011).
[34]H. Wang, A. Chroneos, C. A. Londos, E. N. Sgourou, and U. Schwingenschlögl, Appl. Phys. Lett. **103**, 052101 (2013).
[35]H. Haesslein, R. Sielemann, and C. Zistl, Phys. Rev. Lett. **80**, 2626 (1998).
[36]S. Brotzmann, H. Bracht, J. Lundsgaard Hansen, A. Nylandsted Larsen, E. Simoen, E. E. Haller, J. S. Christensen, and P. Werner, Phys. Rev. B **77**, 235207 (2008).
[37]A. Chroneos, H. Bracht, R. W. Grimes, and B. P. Uberuaga, Appl. Phys. Lett. **92**, 172103 (2008).
[38]C. Janke, R. Jones, S. Öberg, and P. R. Briddon, J. Mater. Sci.: Mater. Electron. **18**, 775 (2007).
[39]A. Chroneos, B. P. Uberuaga, and R. W. Grimes, J. Appl. Phys. **102**, 083707 (2007).
[40]S. Uppal, A. F. W. Willoughby, J. M. Bonar, A. G. R. Evans, N. E. B. Cowern, R. Morris, and M. G. Dowsett, J. Appl. Phys. **90**, 4293 (2001).
[41]C. O. Chui, K. Gopalakrishnan, P. B. Griffin, J. D. Plummer, and K. C. Saraswat, Appl. Phys. Lett. **83**, 3275 (2003).
[42]P. Dorner, W. Gust, A. Lodding, H. Odelius, and B. Predel, Acta Metall. **30**, 941 (1982).
[43]P. Dorner, W. Gust, A. Lodding, H. Odelius, B. Predel, and U. Roll, Z. Metallkd. **73**, 325 (1982).
[44]U. Södervall, H. Odelius, A. Lodding, U. Roll, B. Predel, W. Gust, and P. Dorner, Philos. Mag. A **54**, 539 (1986).
[45]R. Kube, H. Bracht, A. Chroneos, M. Posselt, and B. Schmidt, J. Appl. Phys. **106**, 063534 (2009).
[46]A. Chroneos, R. Kube, H. Bracht, R. W. Grimes, and U. Schwingenschlögl, Chem. Phys. Lett. **490**, 38 (2010).
[47]S. Brotzmann and H. Bracht, J. Appl. Phys. **103**, 033508 (2008).
[48]A. Chroneos, R. W. Grimes, B. P. Uberuaga, and H. Bracht, Phys. Rev. B **77**, 235208 (2008).
[49]H. Tahini, A. Chroneos, R. W. Grimes, U. Schwingenschlögl, and H. Bracht, Appl. Phys. Lett. **99**, 072112 (2011).
[50]H. Letaw, Jr., W. M. Portnoy, and L. Slifkin, Phys. Rev. **102**, 636 (1956).
[51]M. W. Valenta and C. Ramasastry, Phys. Rev. **106**, 73 (1957).
[52]N. A. Stolwijk, W. Frank, J. Hölzl, S. J. Pearton, and E. E. Haller, J. Appl. Phys. **57**, 5211 (1985).
[53]H. Bracht, N. A. Stolwijk, and H. Mehrer, Phys. Rev. B **43**, 14465 (1991).
[54]H. Bracht, Mater. Sci. Semicond. Process. **7**, 113 (2004).
[55]H. Bracht, E. E. Haller, and R. Clark-Phelps, Phys. Rev. Lett. **81**, 393 (1998).
[56]Y. Shimizu, M. Uematsu, and K. M. Itoh, Phys. Rev. Lett. **98**, 095901 (2007).
[57]R. Kube, H. Bracht, E. Hüger, H. Schmidt, J. Lundsgaard Hansen, A. Nylandsted Larsen, J. W. Ager III, E. E. Haller, T. Geue, and J. Stahn, Phys. Rev. B **88**, 085206 (2013).
[58]A. Seeger and K. P. Chik, Phys. Status Solidi **29**, 455 (1968).
[59]N. E. B. Cowern, S. Simdyankin, C. Ahn, N. S. Bennett, J. P. Goss, J.-M. Hartmann, A. Pakfar, S. Hamm, J. Valentin, E. Napolitani, D. De Salvador, E. Bruno, and S. Mirabella, Phys. Rev. Lett. **110**, 155501 (2013).
[60]T. Südkamp, H. Bracht, G. Impellizzeri, J. Lundsgaard Hansen, A. Nylandsted Larsen, and E. E. Haller, Appl. Phys. Lett. **102**, 242103 (2013).
[61]A. Mesli, L. Dobaczewski, K. Bonde Nielsen, Vl. Kolkovsky, M. Christian Petersen, and A. Nylandsted Larsen, Phys. Rev. B **78**, 165202 (2008).
[62]J. Coutinho, R. Jones, V. J. B. Torres, M. Barroso, S. Öberg, and P. R. Briddon, J. Phys.: Condens. Matter **17**, L521 (2005).
[63]A. Satta, E. Simoen, T. Janssens, T. Clarysse, B. De Jaeger, A. Benedetti, I. Hoflijk, B. Brijs, M. Meuris, and W. Vandervorst, J. Electrochem. Soc. **153**, G229 (2006); S. Satta, T. Janssens, T. Clarysse, E. Simoen, M. Meuris, A. Benedetti, I. Hoflijk, B. De Jaeger, C. Demeurisseand, and W. Vandervorst, J. Vac. Sci. Technol. B **24**, 494 (2006).
[64]M. Posselt, B. Schmidt, W. Anwand, R. Grötzschel, V. Heera, A. Mücklich, H. Hortenbach, S. Gennaro, M. Bersani, D. Giubertoni, A. Möller, and H. Bracht, J. Vac. Sci. Technol. B **26**, 430 (2008).
[65]B. C. Johnson, P. Gortmaker, and J. C. McCallum, Phys. Rev. B **77**, 214109 (2008).
[66]S. Koffel, N. Cherkashin, F. Houdellier, M. J. Hytch, G. Benassayag, P. Scheiblin, and A. Claverie, J. Appl. Phys. **105**, 126110 (2009).
[67]S. Mayburg, Phys. Rev. **95**, 38 (1954).
[68]J. A. Hiraki, J. Phys. Soc. Jpn. **21**, 34 (1966).
[69]D. Shaw, Phys. Status Solidi B **72**, 11 (1975).
[70]M. Dionízio Moreira, R. H. Miwa, and P. Venezuela, Phys. Rev. B **70**, 115215 (2004).
[71]A. Carvalho, R. Jones, C. Janke, J. P. Goss, P. R. Briddon, J. Coutinho, and S. Öberg, Phys. Rev. Lett. **99**, 175502 (2007).
[72]S. Schneider, H. Bracht, J. N. Klug, J. Lundsgaard Hansen, A. Nylandsted Larsen, D. Bougeard, and E. E. Haller, Phys. Rev. B **87**, 115202 (2013).
[73]H. Bracht, Phys. Rev. B **75**, 035210 (2007).
[74]F. C. Frank and D. Turnbull, Phys. Rev. **104**, 617 (1956).
[75]L. Pelaz, M. Jaraiz, G. H. Gilmer, H.-J. Gossmann, C. S. Rafferty, D. J. Eaglesham, and J. M. Poate, Appl. Phys. Lett. **70**, 2285 (1997).

[76]P. A. Stolk, H.-J. Gossmann, D. J. Eaglesham, D. C. Jacobson, C. S. Rafferty, G. H. Gilmer, M. Jaraíz, J. M. Poate, H. S. Luftman, and T. E. Haynes, J. Appl. Phys. **81**, 6031 (1997).
[77]P. Pichler, in Silicon Front-End Junction Formation Technologies, edited by Daniel F. Downey, Mark E. Law, Alain Claverie, Michael J. Rendon (Mater. Res. Soc. Symp. Proc., 2002), Vol. 717, p. C3.1.1.
[78]H. Bracht, H. H. Silvestri, I. D. Sharp, and E. E. Haller, Phys. Rev. B **75**, 035211 (2007).
[79]E. Vainonen-Ahlgren, T. Ahlgren, J. Likonen, S. Lehto, J. Keinonen, W. Li, and J. Haapamaa, Appl. Phys. Lett. **77**, 690 (2000).
[80]P. Tsouroutas, D. Tsoukalas, I. Zergioti, N. Cherkashin, and A. Claverie, J. Appl. Phys. **105**, 094910 (2009).
[81]D. P. Brunco, B. De Jaeger, G. Eneman, J. Mitard, G. Hellings, A. Satta, V. Terzieva, L. Souriau, F. E. Leys, G. Pourtois, M. Houssa, G. Winderickx, E. Vrancken, S. Sioncke, K. Opsomer, G. Nicholas, M. Caymax, A. Stesmans, J. Van Steenbergen, P. W. Mertens, M. Meuris, and M. M. Heyns, J. Electrochem. Soc. **155**, H552 (2008).
[82]T. Canneaux, D. Mathiot, J.-P. Ponpon, and Y. Leroy, Thin Solid Films **518**, 2394 (2010).
[83]M. S. Carroll and R. Koudelka, Semicond. Sci. Technol. **22**, S164 (2007).
[84]Y. Cai, R. Camacho-Aguilera, J. T. Bessette, L. C. Kimerling, and J. Michel, J. Appl. Phys. **112**, 034509 (2012).
[85]I. Riihimäki, A. Virtanen, S. Rinta-Anttila, P. Pusa, J. Räisänen, and ISOLDE Collaboration, Appl. Phys. Lett. **91**, 091922 (2007).
[86]S. Uppal, A. F. W. Willoughby, J. M. Bonar, N. E. B. Cowern, T. Grasby, R. J. H. Morris, and M. G. Dowsett, J. Appl. Phys. **96**, 1376 (2004).
[87]S. Mirabella, D. De Salvador, E. Napolitani, E. Bruno, and F. Priolo, J. Appl. Phys. **113**, 031101 (2013).
[88]C. Wündisch, M. Posselt, B. Schmidt, V. Heera, T. Schumann, A. Mücklich, R. Grötzschel, W. Skorupa, T. Clarysse, E. Simoen, and H. Hortenbach, Appl. Phys. Lett. **95**, 252107 (2009).
[89]G. Hellings, E. Rosseel, E. Simoen, D. Radisic, D. H. Petersen, O. Hansen, P. F. Nielsen, G. Zschatzsch, A. Nazir, T. Clarysse, W. Vandervorst, T. Y. Hoffmann, and K. De Meyer, Electrochem. Solid-State Lett. **14**, H39 (2011); E. Bruno, G. G. Scapellato, G. Bisognin, E. Carria, L. Romano, A. Carnera, and F. Priolo, J. Appl. Phys. **108**, 124902 (2010).
[90]J. Huang, N. Wu, Q. Zhang, C. Zhu, A. A. O. Tay, G. Chen, and M. Hong, Appl. Phys. Lett. **87**, 173507 (2005).
[91]C. O. Chui, L. Kulig, J. Moran, W. Tsai, and K. C. Saraswat, Appl. Phys. Lett. **87**, 091909 (2005).
[92]G. Luo, C. C. Cheng, C. Y. Huang, S. L. Hsu, C. H. Chien, W. X. Ni, and C. Y. Chang, Electron. Lett. **41**, 1354 (2005).
[93]E. E. Haller, W. L. Hansen, P. Luke, R. McMurray, and B. Jarrett, IEEE Trans. Nucl. Sci. **29**, 745 (1982).
[94]A. Krukau, O. Vydrov, A. Izmaylov, and G. Scuseria, J. Chem. Phys. **125**, 224106 (2006).
[95]S. M. Sze, *The Physics of Semiconductor Devices* (Wiley, New York, 2006).
[96]S. Lany and A. Zunger, Modell. Simul. Mater. Sci. Eng. **17**, 084002 (2009).
[97]S. Lany and A. Zunger, Phys. Rev. B **78**, 235104 (2008).
[98]S. M. Hu, Phys. Status Solidi B **60**, 595 (1973).
[99]H. Höhler, N. Atodiresei, K. Schroeder, R. Zeller, and P. Dederichs, Phys. Rev. B **71**, 35212 (2005).
[100]J. Vanhellemont and E. Simoen, Mater. Sci. Semicond. Process. **15**, 642 (2012).
[101]I. A. Trumbore, Bell Syst. Tech. J. **39**, 205 (1960).
[102]V. E. Borisenko and S. G. Yudin, Phys. Status Solidi A **101**, 123 (1987).
[103]A. Chroneos, R. W. Grimes, B. P. Uberuaga, S. Brotzmann, and H. Bracht, Appl. Phys. Lett. **91**, 192106 (2007).
[104]S. Satta, E. Simoen, R. Duffy, T. Janssens, T. Clarysse, A. Benedetti, M. Meuris, and W. Vandervorst, Appl. Phys. Lett. **88**, 162118 (2006).
[105]F. A. Kröger and V. J. Vink, *in Solid State Physics*, edited by F. Seitz and D. Turnbull (Academic, New York, 1956), Vol. 3, p. 307.
[106]D. W. Lawther, U. Myler, P. J. Simpson, P. M. Rousseau, P. B. Griffin, and J. D. Plummer, Appl. Phys. Lett. **67**, 3575 (1995).
[107]S. Solmi, D. Nobili, and J. Shao, J. Appl. Phys. **87**, 658 (2000).
[108]J. Xie and S. P. Chen, J. Appl. Phys. **87**, 4160 (2000).
[109]A. Satta, E. Albertazzi, G. Lulli, and L. Colombo, Phys. Rev. B **72**, 235206 (2005).
[110]R. Pinacho, M. Jaraiz, P. Castrillo, I. Martin-Bragado, J. E. Rubio, and J. Barbolla, Appl. Phys. Lett. **86**, 252103 (2005).
[111]A. Chroneos, R. W. Grimes, H. Bracht, and B. P. Uberuaga, J. Appl. Phys. **104**, 113724 (2008).
[112]A. Chroneos, R. W. Grimes, and H. Bracht, J. Appl. Phys. **106**, 063707 (2009).
[113]S. Boninelli, G. Impellizzeri, F. Priolo, E. Napolitani, and C. Spinella, Nucl. Instrum. Methods Phys. Res. B **282**, 21 (2012).
[114]G. Impellizzeri, E. Napolitani, S. Boninelli, J. P. Sullivan, J. Roberts, S. J. Buckman, S. Ruffell, F. Priolo, and V. Privitera, ECS J. Solid State Sci. Technol. **1**, Q44 (2012).
[115]V. V. Emtsev, Jr., C. A. J. Ammerlaan, V. V. Emtsev, G. A. Oganesyan, B. A. Andreev, D. F. Kuritsyn, A. Misiuk, B. Surma, and C. A. Londos, Phys. Status Solidi B **235**, 75 (2003); A. Misiuk, J. Bak-Misiuk, A. Barcz, A. Romano-Rodriguez, I. V. Antonova, V. P. Popov, C. A. Londos, and J. Jun, Int. J. Hydrogen Energy **26**, 483 (2001).
[116]M. L. David, E. Simoen, C. Clays, V. B. Neimash, M. Kra'sko, A. Kraitchinscii, V. Voytovych, A. Kabaldin, and J. F. Barbot, J. Phys.: Condens. Matter **17**, S2255 (2005).
[117]A. Chroneos, C. A. Londos, and E. N. Sgourou, J. Appl. Phys. **110**, 093507 (2011).
[118]A. Chroneos, C. A. Londos, E. N. Sgourou, and P. Pochet, Appl. Phys. Lett. **99**, 241901 (2011).
[119]E. N. Sgourou, D. Timerkaeva, C. A. Londos, D. Aliprantis, A. Chroneos, D. Caliste, and P. Pochet, J. Appl. Phys. **113**, 113506 (2013); C. A. Londos, E. N. Sgourou, D. Timerkaeva, A. Chroneos, P. Pochet, and V. V. Emtsev, J. Appl. Phys. **114**, 113504 (2013).
[120]W. Scorupa and R. A. Yankov, Mater. Chem. Phys. **44**, 101 (1996).
[121]R. I. Scace and G. A. Slack, J. Chem. Phys. **30**, 1551 (1959).
[122]E. E. Haller, W. L. Hansen, and F. S. Goulding, Adv. Phys. **30**, 93 (1981).
[123]P. A. Stolk, H. J. Gossmann, D. J. Eaglesham, and J. M. Poate, Mater. Sci. Eng., B **36**, 275 (1996).
[124]B. J. Pawlak, R. Duffy, T. Janssens, W. Vandervorst, S. B. Felch, E. J. H. Collart, and N. E. B. Cowern, Appl. Phys. Lett. **89**, 062102 (2006).
[125]A. Chroneos, Semicond. Sci. Technol. **26**, 095017 (2011).
[126]A. Brelot and J. Charlemagne, Radiat. Eff. **9**, 65 (1971).
[127]M. L. David, E. Simoen, C. Clays, V. B. Neimash, N. Kra'sko, A. Kraitchinscii, V. Voytovych, V. Tishchenko, and J. F. Barbot, in *The Proc. High Purity Silicon VIII*, The Electrochem. Soc. Ser Proc. (2004), Vol. 2004–2005, p. 395.
[128]C. A. Londos, E. N. Sgourou, and A. Chroneos, J. Appl. Phys. **112**, 123517 (2012).
[129]G. D. Watkins and J. W. Corbett, Phys. Rev. **121**, 1001 (1961).
[130]H. A. Tahini, A. Chroneos, R. W. Grimes, U. Schwingenschlögl, and H. Bracht, Phys. Chem. Chem. Phys. **15**, 367 (2013).
[131]H. A. Tahini, A. Chroneos, R. W. Grimes, and U. Schwingenschlögl, Appl. Phys. Lett. **99**, 162103 (2011).
[132]G. Thareja, S. L. Cheng, T. Kamins, K. Saraswat, and N. Nishi, IEEE Electron Device Lett. **32**, 608 (2011).
[133]J. Kim, S. W. Bedell, and D. K. Sadana, Appl. Phys. Lett. **98**, 082112 (2011).
[134]H. A. Tahini, A. Chroneos, R. W. Grimes, and U. Schwingenschlögl, J. Appl. Phys. **113**, 073704 (2013).
[135]X. D. Pi, C. P. Burrows, and P. G. Coleman, Phys. Rev. Lett. **90**, 155901 (2003).
[136]F. Bernardi, J. H. R. dos Santos, and M. Behar, Phys. Rev. B **76**, 033201 (2007).
[137]S. Boninelli, G. Impellizzeri, S. Mirabella, F. Priolo, E. Napolitani, N. Cherkashin, and F. Cristiano, Appl. Phys. Lett. **93**, 061906 (2008).
[138]C. G. Van de Walle, F. R. McFeely, and S. T. Pantelides, Phys. Rev. Lett. **61**, 1867 (1988).
[139]M. Diebel and S. T. Dunham, Phys. Rev. Lett. **93**, 245901 (2004).
[140]G. M. Lopez, V. Fiorentini, G. Impellizzeri, S. Mirabella, and E. Napolitani, Phys. Rev. B **72**, 045219 (2005).
[141]V. Fiorentini and G. M. Lopez, Phys. Rev. Lett. **96**, 039601 (2006).
[142]G. M. Lopez and V. Fiorentini, Appl. Phys. Lett. **89**, 092113 (2006).
[143]S. A. Harrison, T. F. Edgar, and G. S. Hwang, Phys. Rev. B **74**, 121201(R) (2006).
[144]W. S. Jung, J. H. Park, A. Nainani, D. Nam, and K. C. Saraswat, Appl. Phys. Lett. **101**, 072104 (2012).
[145]H. Bracht, S. Schneider, J. N. Klug, C. Y. Liao, J. Lundsgaard Hansen, E. E. Haller, A. Nylandsted Larsen, D. Bougeard, M. Posselt, and C. Wündisch, Phys. Rev. Lett. **103**, 255501 (2009).
[146]S. Schneider and H. Bracht, Appl. Phys. Lett. **98**, 014101 (2011).
[147]H. Bracht, J. Fage Pedersen, N. Zangenberg, A. Nylandsted Larsen, E. E. Haller, G. Lulli, and M. Posselt, Phys. Rev. Lett. **91**, 245502 (2003).
[148]H. Bracht, "Defect engineering in germanium," Phys. Status Solidi. A (published online).

[149]S. Schneider, Ph.D. dissertation, Münster University, 2012.
[150]D. Alloyeau, B. Freitag, S. Dag, L. W. Wang, and C. Kisielowski, Phys. Rev. B **80**, 014114 (2009).
[151]N. E. B. Cowern, K. T. F. Janssen, G. F. A. van de Walle, and D. J. Gravesteijn, Phys. Rev. Lett. **65**, 2434 (1990).
[152]G. G. Scapellato, S. Boninelli, E. Napolitani, E. Bruno, A. J. Smith, S. Mirabella, M. Mastromatteo, D. De Salvador, R. Gwilliam, C. Spinella, A. Carnera, and F. Priolo, Phys. Rev. B **84**, 024104 (2011).
[153]E. Kamiyama, K. Sueoka, and J. Vanhellemont, J. Appl. Phys. **111**, 083507 (2012).
[154]H. Gang and H. A. Atwater, Appl. Phys. Lett. **68**, 664 (1996).
[155]A. V. G. Chizmeshya, M. R. Bauer, and J. Kouvetakis, Chem. Mater. **15**, 2511 (2003).
[156]R. Roucka, J. Tolle, C. Cook, A. V. G. Chizmeshya, J. Kouvetakis, V. D'Costa, J. Menendez, and Z. D. Chen, Appl. Phys. Lett. **86**, 191912 (2005).
[157]J. Kouvetakis, J. Menendez, and A. V. G. Chizmeshya, Annu. Rev. Mater. Res. **36**, 497 (2006).
[158]A. Chroneos, C. Jiang, R. W. Grimes, U. Schwingenschlögl, and H. Bracht, Appl. Phys. Lett. **95**, 112101 (2009).